Exact Solutions for Rectangularly Shielded Lines by the Carleman–Vekua Method

JOHN G. FIKIORIS AND JOHN L. TSALAMENGAS, MEMBER, IEEE

***Abstract*—Exact solutions for the field of the TEM mode of rectangularly shielded round or strip conductors are obtained by solving linear, singular integral equations. There are no limitations on the dimensions or the proximity of the conductors to the shield. Here only round conductors are considered; printed microstrip conductors are analyzed in further publications. The kernel of the integral equation in such problems is the Green's function *G* of a line source inside the shield, possessing a logarithmic singularity near the source point. In a series of recent papers the authors have developed new expansions for *G*, in which the singular and certain other terms are extracted in closed form out of *G* and the remaining, nonsingular part is then reexpanded into series converging uniformly everywhere and very rapidly (exponentially) near the source point. These new expansions for *G* are particularly suited for the exact solution of the singular integral equation of round shielded conductors by the Carleman–Vekua method, otherwise known as the method of regularization by solving the dominant equation. This leads to strongly convergent solutions for the field of the mode even when the conductors are large or very near the shield. Questions of integrability of nonuniformly convergent series do not arise. Characteristic values of the shielded lines, evaluated by summing a few terms, have been checked against existing approximate results and field plots are shown in the case of close proximity. Due to the exponential convergence of the kernel expansion it is possible to provide useful, closed-form expressions for the characteristic impedance of the line. The accuracy of such formulas is shown to be amply adequate for most practical situations.**

I. Introduction

RECTANGULARLY SHIELDED round conductors, striplines, and printed microstrips are widely used guiding structures in the microwave band [1]–[5]. The literature is extensive; here, we confine ourselves to a few references that will be needed for comparison later. From the mathematical standpoint such structures constitute problems involving boundaries of different shapes and boundary conditions. In a series of recent papers [6]–[9] the authors have developed an exact analytical approach for the treatment of such problems. The practical importance of this approach, if one wishes to disregard its power of providing exact analytical results for quantities such as field-function distributions, is that it is not limited by the dimensions or the proximity of the conductors relative to the shield and that, in most practical situations, it provides very accurate results in closed form for quantities such as the characteristic impedance of the line. Such results and expressions can be very useful in the design of TEM filters and couplers [3], [4].

In this paper only round conductors of radius d will be considered, as shown in Figs. 1 and 2. They are completely shielded by a rectangular $a \times b$ shield. Striplines, and, most important from the practical standpoint, shielded microstrip lines can also be treated by extensions of the same general approach [8], [9]; the latter, involving substrates of different dielectric constants, require appropriate expansions for the relevant Green's function. Such expansions have also been developed [8].

Crucial to the whole analytical approach is the availability of rapidly and uniformly convergent eigenfunction expansions for the Green's function G of the configuration. The G function constitutes the kernel of the integral equation, which is of the Hilbert type for round conductors and of the Carleman type for strip ones [9]. Its solution follows the Carleman–Vekua method, otherwise known as the method of regularization by solving the dominant equation [10].

Existing expansions for G suffer from two serious defects: they do not converge uniformly in their region of validity, exhibiting a slow and conditional convergence near the singular point and, what is worse, they change expression when the field point moves past the source point [7]. For such reasons they are unsuited for the solution of integral equations, in which values of G at the source point do appear inside the integral.

Another approach based on integral equations should also be mentioned here. It was developed initially by Lewin [11] and used by Mittra and Itoh [12] to treat waveguide problems (Helmholtz instead of Laplace's equation) in shielded microstrip configurations. They do not follow the Carleman–Vekua method to solve the integral equation, but they too end up with rapidly converging series solutions. It is not clear how they would face the problem of proximity. The Carleman–Vekua method used herein treats initially all terms of the integral equation other than the singular as terms containing known functions [10]. Using the well-known inversion formula of Hilbert (or Carleman), it then transforms the integral equation into a Fredholm-type nonsingular equation; this is then solved using the appropriate expansions of G. There are two main advantages: all integrals involved in the process can be evaluated exactly by contour integration and the final solution reflects the same convergence

Manuscript received July 15, 1987; revised October 12, 1987.
The authors are with the Department of Electrical Engineering, National Technical University of Athens, Athens, Greece.
IEEE Log Number 8719208.

0018-9480/88/0400-0659$01.00 ©1988 IEEE

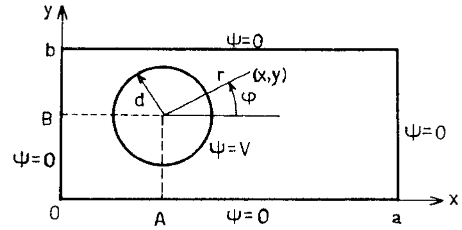

Fig. 1. Configuration of shielded single conductor.

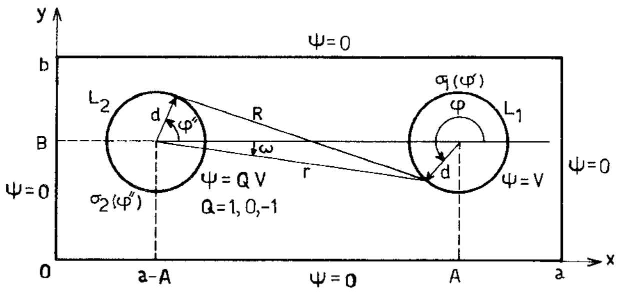

Fig. 2. Configuration of two-conductor shielded line.

properties that characterize the expansions of the kernel function G. Another way of explaining the usefulness of the Carleman–Vekua method is to consider it as a smoothing procedure for solving an ill-posed problem such as a first-kind singular integral equation, similar to equation (23) below.

II. Rapidly Convergent Green's Function Expansion and the Integral Equation

All field quantities of the TEM mode in the shielded-line structures shown in Figs. 1 and 2 can be expressed in terms of a two-dimensional harmonic Green's function $G(x, y; x', y')$ of a line source at (x', y') inside a rectangular conducting shield; this G function satisfies the boundary value problem

$$\frac{\partial^2 G}{\partial x^2}+\frac{\partial^2 G}{\partial y^2}=-2\pi\delta(x-x')\delta(y-y')$$

$$0 \leqslant x,\ x' \leqslant a,\ 0 \leqslant y,\ y' \leqslant b \quad (1)$$

$$G(0, y; x', y')=G(a, y; x', y')$$

$$=G(x,0; x', y')=G(x, b; x', y')=0 \quad (2)$$

where $\delta(x)$ is the delta function. Two new expansions for G have been developed in [7]. The first, obtained by extracting the logarithmic and certain other simple harmonic terms out of G and reexpanding its remaining nonsingular part, contains four series $S_j(x, y; x', y')$ ($j=1,2,3,4$) converging uniformly over the whole region $0 \leqslant x \leqslant a$, $0 \leqslant y \leqslant b$ and exponentially near the source point (x', y'). This new expansion is

$$\begin{aligned}G(x, y; x', y') &= -\frac{1}{2}\ln\left[(x-x')^2+(y-y')^2\right]+S(x, y; x', y')\\ &= -\frac{1}{2}\ln\left[(x-x')^2+(y-y')^2\right]\\ &\quad +1/(2ab)\left\{xy\ln\left[(a-x')^2+(b-y')^2\right]\right.\\ &\quad +(a-x)y\ln\left[x'^2+(b-y')^2\right]\\ &\quad +x(b-y)\ln\left[(a-x')^2+y'^2\right]\\ &\quad \left.+(a-x)(b-y)\ln(x'^2+y'^2)\right\}\\ &\quad +\sum_{j=1}^{4} S_j(x, y; x', y')\end{aligned} \quad (3)$$

where

$$S_1(x, y; x', y')=-\sum_{M=1}^{\infty}\frac{\sin\left(\frac{M\pi x}{a}\right)\sinh\left(\frac{M\pi y}{a}\right)}{M\pi\sinh\left(\frac{M\pi b}{a}\right)}\cdot\left\{2\pi\sin\left(\frac{M\pi x'}{a}\right)\exp\left[-\frac{M\pi}{a}(b-y')\right]+d_M(z_1)\right\} \quad (4)$$

$$z_1=-\frac{\pi}{a}(b-y'-ix')$$

$$S_2(x, y; x', y')=S_1(x, b-y; x', b-y') \quad (5)$$

$$z_2=-\frac{\pi}{a}(y'-ix')$$

$$S_3(x, y; x', y')=-\sum_{M=1}^{\infty}\frac{\sin\left(\frac{M\pi y}{b}\right)\sinh\left(\frac{M\pi x}{b}\right)}{M\pi\sinh\left(\frac{M\pi a}{b}\right)}\cdot\left\{2\pi\sin\left(\frac{M\pi y'}{b}\right)\exp\left[-\frac{M\pi}{b}(a-x')\right]+d_M(z_3)\right\} \quad (6)$$

$$z_3=-\frac{\pi}{b}(a-x'-iy')$$

$$S_4(x, y; x', y')=S_3(a-x, y; a-x', y') \quad (7)$$

$$z_4=-\frac{\pi}{b}(x'-iy')$$

$$d_M(z)=\operatorname{Re}\left\{e^{Mz}\left[E_1(Mz-iM\pi)-E_1(Mz)\right]+e^{-M\bar{z}}\left[E_1(-M\bar{z}-iM\pi)-E_1(-M\bar{z})\right]\right\} \quad (8)$$

the bar indicating the complex conjugate. $E_1(z)$ is the exponential integral function:

$$E_1(z)=\overline{E_1(\bar{z})}=-\gamma-\ln z+Ein(z)$$
$$=\int_z^{\infty}\frac{e^{-t}}{t}\,dt=-\gamma-\ln z-\sum_{n=1}^{\infty}\frac{(-1)^n z^n}{n\cdot n!} \quad (9)$$
$$\arg z<\pi, \quad \gamma=\text{Euler's constant}=0.577215665\cdots$$

$$E_1(z)\underset{|z|\to\infty}{\sim}\frac{e^{-z}}{z}\left(1-\frac{1}{z}+\frac{2!}{z^2}-\frac{3!}{z^2}+\cdots\right), \quad |\arg z|<3\pi/2. \quad (10)$$

Various approximations (asymptotic, continuous fraction, etc.) for $E_1(z)$ and for real or complex z, as well as differentiation and integration formulas and useful recursive relations, can be found in [13].

When the field point (x, y) approaches the source point (x', y') the behavior of G, as given in (3), is well described by its dominant logarithmic term. The series expansions S_j $(j=1,2,3,4)$ converge rapidly, in general, in the neighborhood of (x', y'). This can be deduced from the behavior of their general term as $M\to\infty$. Thus, from (8) we first obtain [7]

$$d_M(z)\underset{M\to\infty}{\sim}\frac{2}{M^2}\operatorname{Re}\left[\frac{z^2}{|z|^4}-(-1)^M\frac{(z-i\pi)^2}{|z-i\pi|^4}\right]+0(1/M^3) \quad (11)$$

and the absolute value of the general term of, say, S_3 is less than

$$\frac{2}{M}\exp\left[-\frac{M\pi}{b}(2a-x-x')\right]+\frac{2}{\pi M^3}\exp\left[-\frac{M\pi}{b}(a-x)\right]$$
$$\cdot\left|\operatorname{Re}\left[\frac{z_3^2}{|z_3|^4}-(-1)^M\frac{(z_3-i\pi)^2}{|z_3-i\pi|^4}\right]+0(1/M)\right|$$

as $M\to\infty$. Similar relations can be found for S_1, S_2, S_4.

The first part decays exponentially with M and, in addition, varies as $1/M$. When both x and x' are very near a, the exponential decay weakens and this, as discussed in [7], is due to the influence of the image line source at $x''=2a-x'$ with respect to the boundary $x=a$. If another logarithmic term, corresponding to this source, is extracted out of G, another expression for G is obtained with a series part converging rapidly even for $x\cong x'\cong a$. This second expression for G is given below, in (12)–(18), and proves very useful when the inner conductor is placed very near the walls $x=0$ or $x=a$, or, in case of two charged conductors, very near each other along the line $y=B$.

The second part of the general term of S_3 varies at least as $1/M^3$ and decays exponentially unless $x=a$. Even for $x=a$ the convergence is uniform, of the other $1/M^3$. The convergence of this second part fails only when z_3 or $z_3-i\pi$ approaches zero, i.e., when $x'\cong a$ and $y'\cong 0$ or $y'\cong b$. In other words, when the source point (x', y') is very near one of the two shield corners on the right. This situation may be remedied by extracting out of G three additional logarithmic terms corresponding to the image sources around the 90° corner [7]. With round conductors of nonvanishing radius, this situation does not become critical.

The second expression for G, in which two more logarithmic terms corresponding to image sources at $x''=2a-x'$ and $x'''=-x'$ (i.e., with respect to the walls $x=a$ and $x=0$) are extracted, is

$$G(x,y;x',y')=-\frac{1}{2}\ln\left[(x-x')^2+(y-y')^2\right]$$
$$+\frac{1}{2}\ln\left[(x+x'-2a)^2+(y-y')^2\right]$$
$$+\frac{1}{2}\ln\left[(x+x')^2+(y-y')^2\right]$$
$$-\frac{1}{2ab}\Big\{(a-x)(b-y)\cdot\ln\left[(2a-x')^2+y'^2\right]$$
$$+x(b-y)\ln\left[(a+x')^2+y'^2\right]$$
$$+(a-x)y\ln\left[(2a-x')^2+(b-y')^2\right]$$
$$+xy\ln\left[(a+x')^2+(b-y')^2\right]\Big\}$$
$$+\sum_{j=1}^{4}S_j^0(x,y;x',y') \quad (12)$$

$$S_1^0(x,y;x',y')=\sum_{M=1}^{\infty}\frac{\sin\left(\frac{M\pi x}{a}\right)\sinh\left(\frac{M\pi y}{a}\right)}{M\pi\sinh\left(\frac{M\pi b}{a}\right)}\cdot\left\{D_M(w_1)-2\pi\sin\left(\frac{M\pi x'}{a}\right)\cdot\exp\left[-\frac{M\pi}{a}(b-y')\right]\right\} \quad (13)$$

$$S_2^0(x,y;x',y')=S_1^0(x,b-y;x',b-y') \quad (14)$$

$$S_3^0(x,y;x',y')=\sum_{M=1}^{\infty}\frac{\sin\left(\frac{M\pi y}{b}\right)\sinh\left(\frac{M\pi x}{b}\right)}{M\pi\sinh\left(\frac{M\pi a}{b}\right)}\cdot\left\{d_M(w_3)+2\pi\sin\left(\frac{M\pi y'}{b}\right)\cdot\exp\left[-\frac{M\pi}{b}(a+x')\right]\right\} \quad (15)$$

$$S_4^0(x,y;x',y')=S_3^0(a-x,y;a-x',y') \quad (16)$$

$$w_1=\frac{\pi}{a}(-b+y'+ix') \qquad w_2=\frac{\pi}{a}(-y'+ix')$$
$$w_3=\frac{\pi}{b}(-a-x'+iy') \qquad w_4=\frac{\pi}{b}(-2a+x'+iy') \quad (17)$$

$$D_M(w)=-d_M(w)+d_M(\bar{w})+d_M(\bar{w}+2\pi i). \quad (18)$$

From the definition (18) for $D_M(w)$ and (11), we now get

$$D_M(w) \underset{M\to\infty}{\sim} \frac{2}{M^2}\,\mathrm{Re}\left[\frac{(\bar{w}+i2\pi)^2}{|\bar{w}+i2\pi|^4} - (-1)^M \frac{(\bar{w}+i\pi)^2}{|\bar{w}+i\pi|^4}\right] + 0(1/M^3) \quad (19)$$

and the absolute value of the general term of S_3^0 is less than

$$\frac{2}{M}\exp\left[-\frac{M\pi}{b}(2a-x+x')\right] + \frac{2}{\pi M^3}\exp\left[-\frac{M\pi}{b}(a-x)\right] \cdot \left|\mathrm{Re}\left[\frac{w_3^2}{|w_3|^4} - (-1)^M\frac{(w_3-i\pi)^2}{|w_3-i\pi|^4}\right] + 0(1/M)\right|.$$

The first part converges exponentially for all x, x' (even for $x = x' = a$). In addition, since both $w_3 = (\pi/b)(-a-x'+iy')$ and $w_3 - i\pi = (\pi/b)[-a-x'+i(y'-b)]$ never vanish, the second part varies at least as $1/M^3$ (even at $x = a$) and its convergence does not fail at any of the four corners $x' = 0, a$; $y' = 0, b$. This may be contrasted with the behavior of S_3 near such points, discussed earlier. Similar remarks hold for S_4 and S_4^0. The series S_1, S_1^0 and S_2, S_2^0 suffer only near the walls $y \cong y' \cong b$ and $y \cong y' \cong 0$, respectively, and this behavior also may be corrected by extracting out of G further logarithmic source terms at $y'' = 2b - y'$ and $y''' = -y'$. This is not necessary here, since proximity to the walls $x = 0$, a only will be considered.

The expansions (3) and (12) are very appropriate for the solution of integral equations having G as their kernel on the basis of the Carleman–Vekua method [10]. For round conductors, Figs. 1 and 2, the integral equation is of the Hilbert type. For strip ones the equation is of the Carleman type and can be further extended to the case of printed microstrip lines [8], [9]. The formulation in terms of integral equations is explained in [1]–[3], although the ensuing treatment is strictly numerical or approximate. The problem of close proximity of the conductors to the shield walls and the difficulties it creates are also discussed in [1] and [2]. It will be seen in the following that this problem is faced head on here and, by strictly analytical methods, answers are provided to any required degree of accuracy. Critical in this approach is the proper expansions (3) and, in particular, (12) for G. Extraction of the image term to improve the convergence of the G function has recently been used in scattering problems as well [14].

We start by formulating an integral equation for the single round conductor of Fig. 1. Two-conductor configurations will be considered later, since they constitute rather simple extensions of the main problem of Fig. 1. The basic unknown function is the surface charge distribution $\sigma(\varphi)$ (C/m^2), for $0 \leqslant \varphi \leqslant 2\pi$, on the round conductor surface of radius d and center (A, B) inside the shield $a \times b$. All TEM field quantities can be evaluated by well-known integrals over this (charge distribution) function. Thus, the electrostatic potential function and the field at any point (x, y) or (r, φ) (around the center of the conductor) are

$$\psi(x,y) = \psi(r,\varphi) = \frac{d}{2\pi\epsilon_0}\int_0^{2\pi}\sigma(\varphi')G(x,y;x',y')\,d\varphi' \quad (20)$$

$$\bar{E}(x,y) = \bar{E}(r,\varphi) = -\nabla\psi \quad (21)$$

$$x = A + r\cos\varphi \qquad y = B + r\sin\varphi$$
$$x' = A + d\cos\varphi' \qquad y' = B + d\sin\varphi'. \quad (22)$$

If the potential of the inner conductor is $\psi(d,\varphi) = V$, an integral equation for $\sigma(\varphi)$ is obtained from (20) by letting $r = d$ [10], [15]:

$$\frac{2\pi\epsilon_0}{d}V = \int_0^{2\pi}\sigma(\varphi')G(A+d\cos\varphi, B+d\sin\varphi; A+d\cos\varphi', B+d\sin\varphi')\,d\varphi'. \quad (23)$$

With $r = d$ one gets, from (22), $(x-x')^2+(y-y')^2 = 4d^2\sin^2((\varphi'-\varphi)/2)$ and substituting from (3):

$$-\frac{2\pi\epsilon_0 V}{d} - \ln(2d)\int_0^{2\pi}\sigma(\varphi')\,d\varphi' + \int_0^{2\pi}\sigma(\varphi')S'(\varphi,\varphi')\,d\varphi' = \int_0^{2\pi}\sigma(\varphi')\ln\left|\sin\left(\frac{\varphi'-\varphi}{2}\right)\right|d\varphi' \quad (24)$$

where S' is the value of S when both source and field points fall on the conductor surface:

$$S'(\varphi,\varphi') = S(A+d\cos\varphi, B+d\sin\varphi; A+d\cos\varphi', B+d\sin\varphi'). \quad (25)$$

Equation (24), a singular integral equation with logarithmic kernel, will be transformed to a more conventional type by considering $\sigma(\varphi)$ as the derivative of a new unknown function $W(\varphi)$ [10], [15]:

$$\sigma(\varphi) = W'(\varphi) = dW(\varphi)/d\varphi. \quad (26)$$

Substitution in the dominant (logarithmic) term of (24) only and integration by parts leads, finally, to

$$\frac{2\pi\epsilon_0 V}{d} + 2\pi\sigma_0\ln\left|2d\sin\frac{\varphi}{2}\right| - \int_0^{2\pi}\sigma(\varphi')S'(\varphi,\varphi')\,d\varphi' = \frac{1}{2}\int_0^{2\pi}W(\varphi')\cot\left(\frac{\varphi'-\varphi}{2}\right)d\varphi' \quad (27)$$

$$\sigma_0 = \frac{1}{2\pi}[W(2\pi) - W(0)] = \frac{1}{2\pi}\int_0^{2\pi}\sigma(\varphi)\,d\varphi. \quad (28)$$

III. Solution of the Integral Equation by the Carleman–Vekua Method

One may now recognize (27) as a Hilbert, principal-value, singular integral equation of the first kind [10], [15]. A necessary and sufficient condition for its solution requires further [15, p. 190] that

$$\int_0^{2\pi}\left[\frac{2\pi\epsilon_0 V}{d}+2\pi\sigma_0 \ln\left|2d\sin\frac{\varphi}{2}\right| - \int_0^{2\pi} S'(\varphi,\varphi')\sigma(\varphi')\,d\varphi'\right]d\varphi = 0 \quad (29)$$

whereupon, by Hilbert's inversion formulas, one obtains

$$W(\varphi) = -\frac{1}{2\pi^2}\int_0^{2\pi}\left[\frac{2\pi\epsilon_0 V}{d}+2\pi\sigma_0\left(\ln d+\ln\left|2\sin\frac{\theta}{2}\right|\right) - \int_0^{2\pi}\sigma(\varphi')S'(\theta,\varphi')\,d\varphi'\right]\cdot\cot\left(\frac{\theta-\varphi}{2}\right)d\theta + K \quad (30)$$

with K some constant, whose value is not required, since we need only the function $\sigma(\varphi)$. Using the results [10, pp. 79–80]:

$$\int_0^{2\pi}\cot\frac{\theta-\varphi}{2}\,d\theta = 0$$
$$\int_0^{2\pi}\ln\left|2\sin\frac{\theta}{2}\right|\cot\frac{\theta-\varphi}{2}\,d\theta = \pi(\pi-\varphi) \quad (31)$$

one gets

$$W(\varphi) = -\sigma_0(\pi-\varphi)+\frac{1}{2\pi^2}\int_0^{2\pi}\int_0^{2\pi}\sigma(\varphi')S'(\theta,\varphi')\cdot\cot\frac{\theta-\varphi}{2}\,d\theta\,d\varphi' + K. \quad (32)$$

At this point one may observe that with $S'(\varphi,\varphi')\equiv 0$, i.e., $G=-\frac{1}{2}\ln[(x-x')^2+(y-y')^2]$, (32) yields the correct solution for the unshielded conductor: $W(\varphi)=-\sigma_0(\pi-\varphi)+K$, $\sigma(\varphi)=\sigma_0=$ constant. In this case (29) provides the correct relation between σ_0 and V if the radius r_0, where $\psi(r_0)=0$, is taken into account.

Expanding now $\sigma(\varphi)$ and $W(\varphi)$ into the Fourier series

$$\sigma(\varphi) = \sigma_0 + \sum_{n=1}^{\infty}(a_n\cos n\varphi + b_n\sin n\varphi) \quad (33)$$

$$W(\varphi) = W_0 + \sigma_0\varphi + \sum_{n=1}^{\infty}\frac{1}{n}(a_n\sin n\varphi - b_n\cos n\varphi) \quad (34)$$

substituting them into (32), making use of the orthogonal properties of the $\sin m\varphi$, $\cos m\varphi$ $(m=0,1,2,\cdots)$ functions in combination with the basic relations [10, pp. 79–80]

$$\int_0^{2\pi}\cos m\varphi\cot\frac{\theta-\varphi}{2}\,d\varphi = 2\pi\sin m\theta \qquad (m=0,1,2,\cdots) \quad (35)$$

$$\int_0^{2\pi}\sin m\varphi\cot\frac{\theta-\varphi}{2}\,d\varphi = -2\pi\cos m\theta \qquad (m=1,2,\cdots) \quad (36)$$

and performing first the integration with respect to φ from $\varphi=0$ to 2π, one gets

for $m=0$: $W_0 = -\sigma_0\pi + K$

$$\text{for } m=1,2,\cdots:\quad \left.\begin{matrix}-\dfrac{b_m}{m}\\ -\dfrac{a_m}{m}\end{matrix}\right\} = \frac{1}{2\pi^2}\int_0^{2\pi}\int_0^{2\pi}\begin{bmatrix}\sin m\theta\\ \cos m\theta\end{bmatrix}\cdot S'(\theta,\varphi')\left[\sigma_0+\sum_{n=1}^{\infty}(a_n\cos n\varphi'+b_n\sin n\varphi')\right]d\theta\,d\varphi'. \quad (37)$$

The integrations involved in (37) are carried out in Appendix I. The end result is a system of $2m$ homogeneous linear equations $(m=1,2,\cdots,\infty)$ for the $2m+1$ unknown expansion coefficients σ_0, a_m, b_m having the form

$$-\frac{b_m}{m} = K_{m0}^{sc}\sigma_0 + \sum_{n=1}^{\infty}(K_{mn}^{sc}a_n + K_{mn}^{ss}b_n) \quad (38a)$$

$$-\frac{a_m}{m} = K_{m0}^{cc}\sigma_0 + \sum_{n=1}^{\infty}(K_{mn}^{cc}a_n + K_{mn}^{cs}b_n) \quad (38b)$$

where the K_{mn}^{pq} $(p,q=c,s$ or $s,c)$ are defined below. The required additional nonhomogenous linear equation is provided by substituting (33) into (29). The end result relates the coefficients σ_0, a_n, and b_n to V and has the form

$$\frac{4\epsilon_0 V}{d}+4\sigma_0\ln d = K_{00}^{cc}\sigma_0 + \sum_{n=1}^{\infty}(K_{0n}^{cc}a_n + K_{0n}^{cs}b_n). \quad (39)$$

To get this equation use was made of the integrals [16, p. 584]

$$\int_0^1 \ln(\sin\pi x)\cos(2n\pi x)\,dx = 2\int_0^{1/2}\ln(\sin\pi x)\cos(2n\pi x)\,dx = \begin{cases}-\ln 2, & n=0\\ -\dfrac{1}{2\pi}, & n>0\end{cases} \quad (40a)$$

$$\int_0^{2\pi}\ln\left|2d\sin\frac{\varphi}{2}\right|d\varphi = 2\pi\ln d. \quad (40b)$$

$S'(\varphi,\varphi')$ is defined in (25) and (3)–(9) or (12)–(18). It is important to notice that its dependence on φ and φ' appears in a separated form and facilitates greatly the θ and φ' integrations in (37) and the φ,φ' integrations in (29). Thus, two types of integrals arise from (37):

$$I\left(\begin{matrix}c\\s\end{matrix}, m;\varphi'\right) = \int_0^{2\pi}\begin{pmatrix}\cos m\theta\\ \sin m\theta\end{pmatrix}S'(\theta,\varphi')\,d\theta \qquad (m=0,1,2,\cdots) \quad (41)$$

$$J\left(\begin{matrix}c\\s\end{matrix}, n;\theta\right) = \int_0^{2\pi}S'(\theta,\varphi')\begin{pmatrix}\cos n\varphi'\\ \sin n\varphi'\end{pmatrix}d\varphi' \qquad (n=0,1,2,\cdots). \quad (42)$$

The specific integrals to be evaluated (see Appendix I) are classified as follows:

$$I_1\left({}^c_s, m|A, B\right) = \int_0^{2\pi}\begin{pmatrix}\cos m\theta\\ \sin m\theta\end{pmatrix}(A+d\cos\theta)(B+d\sin\theta)\,d\theta \quad (43)$$

$$I_2\left({}^c_s, m|M;\alpha,\beta,\delta\right) = \int_0^{2\pi}\begin{pmatrix}\cos m\theta\\ \sin m\theta\end{pmatrix}\sin\left[M\pi(\alpha+\delta\cos\theta)\right]\cdot\sinh\left[M\pi(\beta+\delta\sin\theta)\right]d\theta \quad (44)$$

$$J_1\left(\alpha,\beta|n,{}^c_s\right) = \frac{1}{2}\int_0^{2\pi}\ln\left[(\alpha-d\cos\varphi')^2+(\beta-d\sin\varphi')^2\right]\cdot\begin{pmatrix}\cos n\varphi'\\ \sin n\varphi'\end{pmatrix}d\varphi' \quad (45)$$

$$J_2\left(M|n,{}^c_s\right) = \int_0^{2\pi}\sin\left[\frac{M\pi}{a}(A+d\cos\varphi')\right]\cdot\exp\left[-\frac{M\pi}{a}(b-B-d\sin\varphi')\right]\begin{pmatrix}\cos n\varphi'\\ \sin n\varphi'\end{pmatrix}d\varphi' \quad (46)$$

$$J_3\left(M|n,{}^c_s\right) = \int_0^{2\pi}\sin\left[\frac{M\pi}{a}(A+d\cos\varphi')\right]\cdot\exp\left[-\frac{M\pi}{a}(B+d\sin\varphi')\right]\begin{pmatrix}\cos n\varphi'\\ \sin n\varphi'\end{pmatrix}d\varphi' \quad (47)$$

$$J_4\left(M|n,{}^c_s\right) = \int_0^{2\pi}\sin\left[\frac{M\pi}{b}(B+d\sin\varphi')\right]\cdot\exp\left[-\frac{M\pi}{b}(a-A-d\cos\varphi')\right]\begin{pmatrix}\cos n\varphi'\\ \sin n\varphi'\end{pmatrix}d\varphi' \quad (48)$$

$$J_5\left(M|n,{}^c_s\right) = \int_0^{2\pi}\sin\left[\frac{M\pi}{b}(B+d\sin\varphi')\right]\cdot\exp\left[-\frac{M\pi}{b}(A+d\cos\varphi')\right]\begin{pmatrix}\cos n\varphi'\\ \sin n\varphi'\end{pmatrix}d\varphi' \quad (49)$$

$$J_{5+j}\left(M|n,{}^c_s\right) = \int_0^{2\pi}\left\{e^{Mz_j}\left[E_1(Mz_j-iM\pi)-E_1(Mz_j)\right] + e^{-M\bar{z}_j}\left[E_1(-M\bar{z}_j-iM\pi)-E_1(-M\bar{z}_j)\right]\right\}\cdot\begin{pmatrix}\cos n\varphi'\\ \sin n\varphi'\end{pmatrix}d\varphi' \quad (50)$$

with $j=1,2,3,4$ and

$$z_1 = -\frac{\pi}{a}\left[b-B-d\sin\varphi'-i(A+d\cos\varphi')\right] = i\frac{\pi d}{a}\left(e^{-i\varphi'}+\frac{A}{d}+i\frac{b-B}{d}\right) \quad (51a)$$

$$z_2 = -\frac{\pi}{a}\left[B+d\sin\varphi'-i(A+d\cos\varphi')\right] = i\frac{\pi d}{a}\left(e^{i\varphi'}+\frac{A}{d}+i\frac{B}{d}\right) \quad (51b)$$

$$z_3 = -\frac{\pi}{b}\left[a-A-d\cos\varphi'-i(B+d\sin\varphi')\right] = \frac{\pi d}{b}\left(e^{i\varphi'}-\frac{a-A}{d}+i\frac{B}{d}\right) \quad (51c)$$

$$z_4 = -\frac{\pi}{b}\left[A+d\cos\varphi'-i(B+d\sin\varphi')\right] = -\frac{\pi d}{b}\left(e^{-i\varphi'}+\frac{A}{d}-i\frac{B}{d}\right). \quad (51d)$$

In (44) the restriction $0<\delta<|\alpha|,|\beta|$ holds among these three parameters. Also, in (45), $0<d<[\alpha^2+\beta^2]^{1/2}$. Based on the expression (3) for G, the definition of K_{mn}^{pq} in terms of these integrals is the following:

$$\begin{aligned}K_{mn}^{pq} = \frac{1}{\pi^2 ab}&\left[I_1(p,m|A,B)J_1(a-A,b-B|n,q)\right.\\ &-I_1(p,m|A-a,B)J_1(-A,b-B|n,q)\\ &-I_1(p,m|A,B-b)J_1(a-A,-B|n,q)\\ &\left.+I_1(p,m|A-a,B-b)J_1(-A,-B|n,q)\right]\\ &-\sum_{M=1}^{\infty}\left\{\frac{I_2\left(p,m|M;\frac{A}{a},\frac{B}{a},\frac{d}{a}\right)}{M\pi^3\sinh\left(\frac{M\pi b}{a}\right)}\left[2\pi J_2(M|n,q)+\mathrm{Re}\,J_6(M|n,q)\right]\right.\\ &-\frac{I_2\left(p,m|M;\frac{A}{a},\frac{B-b}{a},\frac{d}{a}\right)}{M\pi^3\sinh\left(\frac{M\pi b}{a}\right)}\cdot\left[2\pi J_3(M|n,q)+\mathrm{Re}\,J_7(M|n,q)\right]\\ &-\frac{I_2\left(p,m|iM;\frac{A}{b},\frac{B}{b},\frac{d}{b}\right)}{M\pi^3\sinh\left(\frac{M\pi a}{b}\right)}\cdot\left[2\pi J_4(M|n,q)+\mathrm{Re}\,J_8(M|n,q)\right]\\ &+\left.\frac{I_2\left(p,m|iM;\frac{A-a}{b},\frac{B}{b},\frac{d}{b}\right)}{M\pi^3\sinh\left(\frac{M\pi a}{b}\right)}\cdot\left[2\pi J_5(M|n,q)+\mathrm{Re}\,J_9(M|n,q)\right]\right\}\end{aligned}$$

$$(p,q=c,s \text{ or } s,c),\quad m,n=0,1,2,\cdots. \quad (52)$$

Obviously $K_{0n}^{sq} = K_{m0}^{ps} = 0$. As observed in Appendix I, the series over M in (52) converge at least exponentially with M, unless the inner conductor is placed very near the shielding walls. If (12) instead of (3) is used for G, another expression results for K_{mn}^{pq}, in terms of the same I and J integrals and the integrals P_{mn}^{pq} defined later on in (68) and (A39). This other expression for K_{mn}^{pq}, more appropriate when the conductor is very close to the walls $x = 0, a$, is given in Appendix II.

IV. Evaluation of the Field

At any point (x, y) inside the shield the potential $\psi(x, y)$ and the field $\bar{E}(x, y)$ are evaluated from (20)–(21). Owing to the separated dependence of G on x, y and x', y' the integrals over φ' are exactly the J_j's, for $j = 1$ to 9, defined in (45)–(51). The results are

$$\psi(x, y) = -\frac{d}{2\pi\epsilon_0}\left\{\sigma_0 D(x, y|0, c) + \sum_{n=1}^{\infty}\left[a_n D(x, y|n, c) + b_n D(x, y|n, s)\right]\right\} \tag{53}$$

$$\begin{aligned} D\left(x, y|n, {}^c_s\right) &= J_1\left(x - A, y - B|n, {}^c_s\right) \\ &\quad - \frac{1}{ab}\Big[xyJ_1\left(a - A, b - B|n, {}^c_s\right) \\ &\quad + (a - x)yJ_1\left(-A, b - B|n, {}^c_s\right) \\ &\quad + x(b - y)J_1\left(a - A, -B|n, {}^c_s\right) \\ &\quad + (a - x)(b - y)J_1\left(-A, -B|n, {}^c_s\right)\Big] \\ &\quad + \sum_{M=1}^{\infty}\frac{\sin\left(\frac{M\pi x}{a}\right)\sinh\left(\frac{M\pi y}{a}\right)}{M\pi\sinh\left(\frac{M\pi b}{a}\right)} \cdot\left[2\pi J_2\left(M|n, {}^c_s\right) + \operatorname{Re}J_6\left(M|n, {}^c_s\right)\right] \\ &\quad + \sum_{M=1}^{\infty}\frac{\sin\left(\frac{M\pi y}{a}\right)\sinh\left[\frac{M\pi}{a}(b - y)\right]}{M\pi\sinh\left(\frac{M\pi b}{a}\right)} \cdot\left[2\pi J_3\left(M|n, {}^c_s\right) + \operatorname{Re}J_7\left(M|n, {}^c_s\right)\right] \\ &\quad + \sum_{M=1}^{\infty}\frac{\sin\left(\frac{M\pi y}{b}\right)\sinh\left(\frac{M\pi x}{b}\right)}{M\pi\sinh\left(\frac{M\pi a}{b}\right)} \cdot\left[2\pi J_4\left(M|n, {}^c_s\right) + \operatorname{Re}J_8\left(M|n, {}^c_s\right)\right] \\ &\quad + \sum_{M=1}^{\infty}\frac{\sin\left(\frac{M\pi y}{b}\right)\sinh\left[\frac{M\pi}{b}(a - x)\right]}{M\pi\sinh\left(\frac{M\pi a}{b}\right)} \cdot\left[2\pi J_5\left(M|n, {}^c_s\right) + \operatorname{Re}J_9\left(M|n, {}^c_s\right)\right], \\ &\qquad n = 0, 1, 2, \cdots. \end{aligned} \tag{54}$$

Obviously $D(x, y|0, s) = 0$.

For the field $\bar{E}(x, y) = -\nabla\psi(x, y)$, the partial derivatives $\partial/\partial x$, $\partial/\partial y$ are very simply obtained from (54) for all terms apart from the first, for which, after referring to definitions (A5)–(A7), we have, for $n = 1, 2, \cdots$,

$$\partial J_1\left(x - A, y - B|n, {}^c_s\right)\Big/\partial x = \pi w^{n+2}\left[\begin{pmatrix}\cos n\gamma \\ \sin n\gamma\end{pmatrix}(x - A) - \begin{pmatrix}-\sin n\gamma \\ \cos n\gamma\end{pmatrix}(y - B)\right]\Big/d^2 \tag{55}$$

$$\partial J_1\left(x - A, y - B|n, {}^c_s\right)\Big/\partial y = \pi w^{n+2}\left[\begin{pmatrix}\cos n\gamma \\ \sin n\gamma\end{pmatrix}(y - B) - \begin{pmatrix}-\sin n\gamma \\ \cos n\gamma\end{pmatrix}(x - A)\right]\Big/d^2 \tag{56}$$

$$w = \frac{d}{\left[(x - A)^2 + (y - B)^2\right]^{1/2}} \qquad \gamma = \tan^{-1}\frac{y - B}{x - A}. \tag{57}$$

For $n = 0$

$$\begin{bmatrix}\partial/\partial x \\ \partial/\partial y\end{bmatrix} J_1(x - A, y - B|0, c) = 2\pi w^2\begin{bmatrix}x - A \\ y - B\end{bmatrix}\Big/d^2. \tag{58}$$

V. Two-Conductor Configurations

Such configurations with arbitrary conductor radii and positions lead to a system of integral equations for $\sigma_1(\varphi_1)$ and $\sigma_2(\varphi_2)$. More practical ones consist of conductors of the same radius d, symmetrically placed with respect to the midplane $x = a/2$, as shown in Fig. 2. They are raised to potentials V and QV, with $Q = 1$ implying equal currents and charges, $Q = -1$ opposite ones, and $Q = 0$ the absence of L_2, i.e., the one-conductor configuration of Fig. 1. Because of the symmetry

$$\sigma_2(\varphi') = Q\sigma_1(\pi - \varphi'); \qquad \sigma_1(\varphi') = dW(\varphi')/d\varphi' \tag{59}$$

the potential $\psi(x, y)$ at any point (x, y) exterior to the conductors is

$$\begin{aligned} \psi(x, y) &= \left(\frac{d}{2\pi\epsilon_0}\right)\Big\{-\frac{1}{2}\int_0^{2\pi}\sigma_1(\varphi') \\ &\quad \cdot\ln\left[(x - A - d\cos\varphi')^2 + (y - B - d\sin\varphi')^2\right]d\varphi' \\ &\quad + \int_0^{2\pi}\sigma_1(\varphi')S(x, y; A + d\cos\varphi', B + d\sin\varphi')\,d\varphi' \\ &\quad - \frac{Q}{2}\int_0^{2\pi}\sigma_1(\pi - \varphi'')\ln\left[(x - a + A - d\cos\varphi'')^2\right. \\ &\quad \left.+ (y - B - d\sin\varphi'')^2\right]d\varphi'' + Q\int_0^{2\pi}\sigma_1(\pi - \varphi'') \\ &\quad \cdot S(x, y; a - A + d\cos\varphi'', B + d\sin\varphi'')\,d\varphi''\Big\}. \end{aligned} \tag{60}$$

Letting (x, y) fall on the surface of L_1, i.e., $x = A + d\cos\varphi$, $y = B + d\sin\varphi$, we obtain a singular integral equation with logarithmic kernel for $\sigma_1(\varphi')$ or a Hilbert-type one for $W(\varphi')$. The latter is

$$\frac{2\pi\epsilon_0 V}{d}+2\pi\sigma_0\ln\left|2d\sin\frac{\varphi}{2}\right|-\int_0^{2\pi}\sigma_1(\varphi')S'(\varphi,\varphi')\,d\varphi' +\int_0^{2\pi}Q\sigma_1(\pi-\varphi')\ln R(\varphi,\varphi'')\,d\varphi'' -\int_0^{2\pi}Q\sigma_1(\pi-\varphi'')S''(\varphi,\varphi'')\,d\varphi'' =\frac{1}{2}\int_0^{2\pi}W(\varphi')\cot\left(\frac{\varphi'-\varphi}{2}\right)d\varphi' \quad (61)$$

and reduces to (27) for $Q=0$. σ_0 is defined in (28), $S'(\varphi,\varphi')$ in (25), while

$$R(\varphi,\varphi'')=\left[(2A-a+d\cos\varphi-d\cos\varphi'')^2+d^2(\sin\varphi-\sin\varphi'')^2\right]^{1/2} \quad (62)$$

$$S''(\varphi,\varphi'')=S(A+d\cos\varphi,B+d\sin\varphi;\; a-A+d\cos\varphi'',B+d\sin\varphi''). \quad (63)$$

The necessary and sufficient condition for the solution of (61) now takes the form

$$\int_0^{2\pi}\left[\frac{2\pi\epsilon_0 V}{d}+2\pi\sigma_0\ln\left|2d\sin\frac{\varphi}{2}\right|-\int_0^{2\pi}\sigma_1(\varphi')S'(\varphi,\varphi')\,d\varphi' +Q\int_0^{2\pi}\sigma_1(\pi-\varphi'')\ln R\,d\varphi'' -Q\int_0^{2\pi}\sigma_1(\pi-\varphi'')S''(\varphi,\varphi'')\,d\varphi''\right]d\varphi=0 \quad (64)$$

and Hilbert's inversion formula, along with (31), leads to

$$W(\varphi)=-\sigma_0(\pi-\varphi)+\frac{1}{2\pi^2}\int_0^{2\pi}\left[\int_0^{2\pi}\sigma_1(\varphi')S'(\theta,\varphi')\,d\varphi' -Q\int_0^{2\pi}\sigma_1(\pi-\varphi'')\ln R(\theta,\varphi'')\,d\varphi'' +Q\int_0^{2\pi}\sigma_1(\pi-\varphi'')S''(\theta,\varphi'')\,d\varphi''\right] \cdot\cot\left(\frac{\theta-\varphi}{2}\right)d\theta. \quad (65)$$

Using the expansions (33), (34) and the formulas (35), (36), we get

$$\left.\begin{matrix}-\dfrac{b_m}{m}\\ -\dfrac{a_m}{m}\end{matrix}\right\}=\frac{1}{\pi^2}\int_0^{2\pi}\int_0^{2\pi}\begin{pmatrix}\sin m\theta\\ \cos m\theta\end{pmatrix}\Bigg\{S'(\theta,\varphi') \cdot\left[\sigma_0+\sum_{n=1}^{\infty}(a_n\cos n\varphi'+b_n\sin n\varphi')\right] +Q[S''(\theta,\varphi')-\ln R(\theta,\varphi')]\left[\sigma_0+\sum_{n=1}^{\infty}(-1)^n \cdot(an\cos n\varphi'-b_n\sin n\varphi')\right]\Bigg\}\,d\theta\,d\varphi'. \quad (66)$$

TABLE I

2d/b	a/b	$Z_0(\Omega)$ this work M=1,3	M=5	$Z_0(\Omega)$ from Cristal
0.6	2.1	44.81	44.17	44.1
0.4	1.9	68.86	68.74	68.7
0.2	1.7	109.94	109.91	109.91

$Q=0$, $A=a/2$, $B=b/2$.

Equations (38a), (38b), and (39) follow in identical form. The only change occurs in the definition (54) for K_{mn}^{pq}, which corresponds to the case $Q=0$. For $Q=1$ or -1 we have

$$K_{mn}^{pq}(Q)=K_{mn}^{pq}+Q(-1)^n S_q\left(L_{mn}^{pq}-P_{mn}^{pq}\right) \quad (67)$$

$$S_q=\begin{cases}1 & \text{for } q=c\\ -1 & \text{for } q=s\end{cases}$$

where L_{mn}^{pq} follows from K_{mn}^{pq} in (52) if A is replaced by $a-A$ in all the J integrals (depending on n), while the I integrals (depending on m) remain unchanged. All this is based on expansion (3). Also

$$P_{mn}^{pq}=\frac{1}{\pi^2}\int_0^{2\pi}\int_0^{2\pi}\begin{pmatrix}\cos m\varphi; & p=c\\ \sin m\varphi; & p=s\end{pmatrix} \cdot\ln R(\varphi,\varphi'')\begin{pmatrix}\cos n\varphi''; & q=c\\ \sin n\varphi''; & q=s\end{pmatrix}d\varphi\,d\varphi''. \quad (68)$$

This double integral is also evaluated in Appendix I.

Finally, $\psi(x,y)$ and $\bar{E}(x,y)$ at any point (x,y) follow from (60), which ends up again in the form (53) with the function $D(x,y|n,{}^c_s)$ replaced now by $D(x,y|n,{}^c_s)+Q(-1)^n\binom{1}{-1}H(x,y|n,{}^c_s)$, where H follows from D in (54) if A is replaced everywhere by $a-A$. The partial derivatives $\partial/\partial x$, $\partial/\partial y$ for the field are again very simple to obtain; for the first term J_1 of H we use (55)–(58) with A replaced by $a-A$.

VI. Numerical Results and Comparisons

In Table I we compare numerical results for the characteristic impedance $Z_0=1/cC=\sqrt{\mu\epsilon}\,V/(2\pi d\sigma_0)$ in ohms ($c=1/\sqrt{\mu\epsilon}$ is the velocity of light and $C=q/V=2\pi d\sigma_0/V$ is the capacitance per unit length) of one-conductor configurations ($Q=0$), with $A=a/2$, $B=b/2$, obtained by Cristal [3] and our method. Like ours, Cristal's results are not limited to small-diameter center conductors and were obtained by solving numerically integral equations. His matrix size, 40×40, should be compared with ours $M\times M=1\times1, 3\times3, 5\times5$, where $M=2m+1$ is the truncation number for the unknowns σ_0, a_m, b_m. Our results settle very rapidly to their final values for small M owing to the strong convergence of the (kernel) Green's function expansion. A table of the successive values of σ_0, a_m, b_m, as m increases, is given later on. The agreement with Cristal's results [3] is excellent. The fact that our results do not differ for $M=1$ and $M=3$ is due to the symmetry of the configuration ($A=a/2$, $B=b/2$), which implies $a_1=b_1=0$.

TABLE II

2d/b	s/b*	Chisholm/McDermott		Levy		This work**	
		Q = 1	Q = -1	Q = 1	Q = -1	Q = 1	Q = -1
.354	.176	3.9142	7.5347	3.9153	7.5528	3.9132	7 5494
.400	.226	4.5093	7.5347	4.5080	7.5404	4.5043	7.5388
436	.280	5.0281	7.5347	5.032	7.5501	5.0332	7.5468
.462	.338	5.4731	7.5347	5.4718	7.5371	5.4718	7.5343
.482	.398	5.8497	7.5347	5.8446	7 5339	5.8455	7 5339
.498	.462	6.1648	7.5347	6.1721	7.5436	6.1721	7.5451
.510	.528	6.4257	7.5347	6.4380	7.5514	6.4399	7.5508
.518	.596	6.6404	7.5347	6.6424	7.5371	6.6421	7.5366
.534	.806	7.0727	7.5347	7.0710	7.5359	7.0721	7.5361
.544	1.168	7.3855	7.5347	7.3806	7.5285	7.3819	7.5304
.400	.080	4.1646	11.0783	4.1553	11.2882	4.1651	11.2371
.400	.120	4.2631	9.4595	4.2626	9.5317	4.2634	9.5118
.400	.160	4.3578	8.4935	4.3516	8 5419	4.3579	8.5152
.400	.200	4.4483	7.8478	4.444	7.8652	4.4481	7.8584
.400	.240	4.5340	7.3863	4.5358	7.3982	4.5337	7.3917
.400	.400	4.8273	6.3903	4.8263	6.3914	4.8265	6.3903
.400	.600	5.0826	5.8862	5.0819	5.8848	5.0818	5 8848
.400	.760	5.2134	5.6949	5.2130	5.6946	5.2128	·5.6940

*$s = 2(A-d) - a$.
**$a/b = 20$, $M = 5$–9.

In Table II we compare results for two-conductor configurations, for both $Q=-1$ and $Q=1$, with those of Levy and Chisholm/McDermott [4]. They refer to the normalized capacitance C/ϵ_0 and open guides in the x direction ($a/b=\infty$). We approximated this situation by using $a/b=20$ to obtain our results. The parameter s in [4] is the shortest approach between the conductors, equivalent to $s=2(A-d)-a$ in our case. Levy's results were obtained by a combination of conformal transformation and numerical techniques. Ours were based on matrix sizes between 5×5 and 9×9. The agreement is again excellent. This fact justifies providing a single-term formula (for $m=0$ or $M=1$) for the first coefficient σ_0 of $\sigma(\varphi)$, on which the evaluation of C or Z_0 is based. For conductors not too large or proximities not too close, either to the shield or between them, the following simple formula, obtained from (39) and (67), can be useful in TEM filter or coupler design (for $Q=0,\pm 1$).

$$\sigma_0=\frac{4\epsilon_0 V}{d}\frac{1}{K_{00}^{cc}(Q)-4\ln d}=\frac{4\epsilon_0 V}{d}\frac{1}{K_{00}^{cc}+Q\left(L_{00}^{cc}-P_{00}^{cc}\right)-4\ln d}. \tag{69}$$

Another check on our formulas is provided by observing that the case of Fig. 2 for $Q=-1$ is equivalent to the case of Fig. 1 with a reduced to $a/2$ (perfectly conducting wall at $x=a/2$). In all cases with $Q=-1$ in an $a\times b$ shield, we obtained numerical results identical with those having $Q=0$ in an $(a/2)\times b$ shield. Observe that the function $R(\varphi,\varphi'')$ is 0 for $Q=0$.

Finally, based on the formulas (53) to (58), nine equipotential lines $\psi=0.9-0.8-\cdots-0.1$, between $\psi=1=V$ on the conductor and $\psi=0$ on the shield were plotted

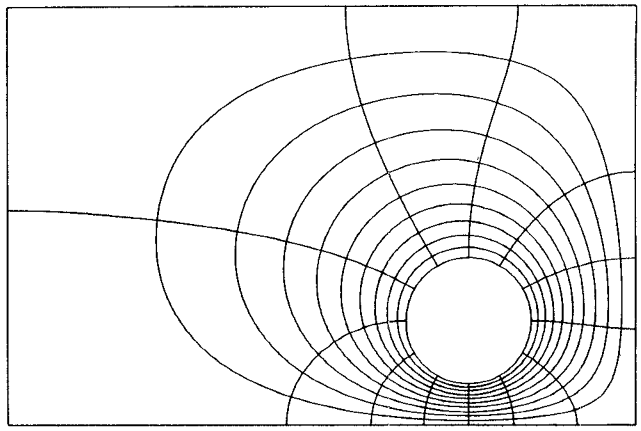

Fig. 3. Equipotential and field lines of shielded single-conductor line.

in Fig. 3, along with field lines starting from $\varphi=0°$ every $30°$ around the conductor. The configuration corresponds to $a=30$, $b=20$, $A=22$, $B=5$, $d=3$. The equipotentials were plotted by varying φ by steps of $2°$ from $\varphi=0°$ to $\varphi=360°$. The algorithms for these evaluations, making use of the methods of bisection and Newton–Raphson for determining roots of complicated equations related to (53)–(58), cannot be described herein for lack of space. As expected, the field between the conductor and the shield in their nearest approach, i.e., for $x\cong 22(=A)$ and $0\leqslant y\leqslant 2(=B-d)$ is almost uniform (almost straight and equispaced equipotential lines). In Table III below the values of $\sigma_0=a_0, a_m, b_m$ in $10^{-12}\cdot$ C/m^2 are given for successive values of matrix size $M=2m+1$, for the configuration of Fig. 3, showing the quick settlement of their values with increasing M. For $m=1$ ($M=3$) the value of $\sigma_0=3.061$ (or C, Z_0) is 0.3 percent off the correct one $\sigma_0=3.0738$. Values of $\sigma(\varphi)$ or the field, however, require use of more a_m, b_m. For the plots of Fig. 3, for example, $m=8$ ($M=17$) were used. In this particular case the use of either (3), (52) or (12), (A42) yields the same a_m, b_m with comparable accuracy. When the conductor approaches either of the walls $x=0$ or $x=a$, the second set, i.e., (12), (A42), (A49), is more advantageous, particularly when $\psi(x,y)$ or $\bar{E}(x,y)$ is evaluated in the region of close proximity. The situation is illustrated in Figs. 4 and 5, in which the equipotentials $\psi=0.9-0.8-\cdots 0.1$ are plotted in the region of close proximity of the conductor to the wall $x=a$. For both figures, $a=30$, $b=20$, $B=5$, $d=3$, while $A=26$ (minimum distance of conductor from wall $a-A-d=1$) in Fig. 4 and $A=26.5$ ($a-A-d=0.5$) in Fig. 5. In Fig. 4(a) and with $m=15$ ($M=31$), the equipotentials $\psi=0.2-0.1$ (very near $x=a$), when evaluated on the basis of (3), (52), (54), instead of turning out smooth, almost straight lines, they tend to oscillate, indicating a lack of accuracy in their computation. This disappears either by using more terms, $m=20$, or by making the evaluation on the basis of (12), (A42), (A49) with fewer terms, $m=15$ or even less, as shown in Fig. 4(b). This result points to the superiority of (12), (A42), (A49) in such situations and can be explained as follows: when x is very near a the series $S_3(x,y;x',y')$ in (4),

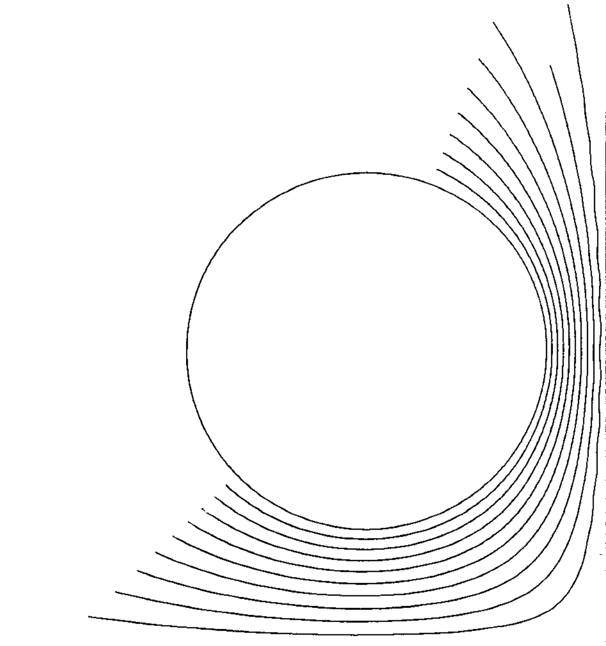

(a)

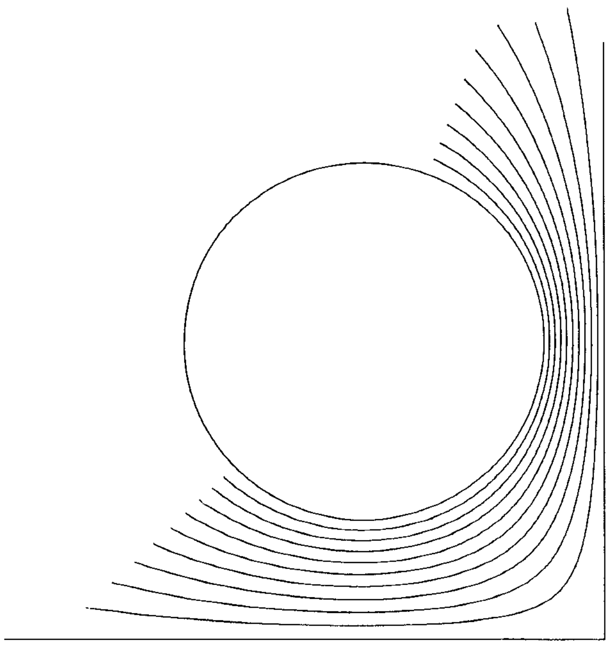

(b)

Fig. 4. Equipotential lines in the region of close proximity between conductor and shielding wall ($a-A-d=1$). (a) On the basis of (3) and (54) with $m=15$. (b) On the basis of (3), (54) with $m=20$ or on the basis of (12) and (A49) with $m=15$.

(3) or $S_3^0(x, y; x', y')$ in (15), (12) lose their exponential decay with M, arising from the fraction $\sinh(M\pi x/b)/\sinh(M\pi a/b)$, and the same thing happens with the corresponding terms in (56) and (A49) for $D(x, y|n, {}^c_s)$, when evaluating $\psi(x, y)$ in (53). However, the values of $G(x, y; x', y')$ and $D(x, y; n, {}^c_s)$ at such points, based on (12), (A49) do not depend so critically on the series over M, but on the closed-form terms arising from the extraction of the line source and its image. So they "settle down" to their "final" values faster than when evaluated on the basis of (3), (54), in which the series over M, including the influence of the nearby image source, affects the total value of G or D in a more direct way, thus requiring more terms. At other points (x, y) away from the boundary or when the inner conductor is not close to it, both expansions are equivalent as far as convergence is concerned.

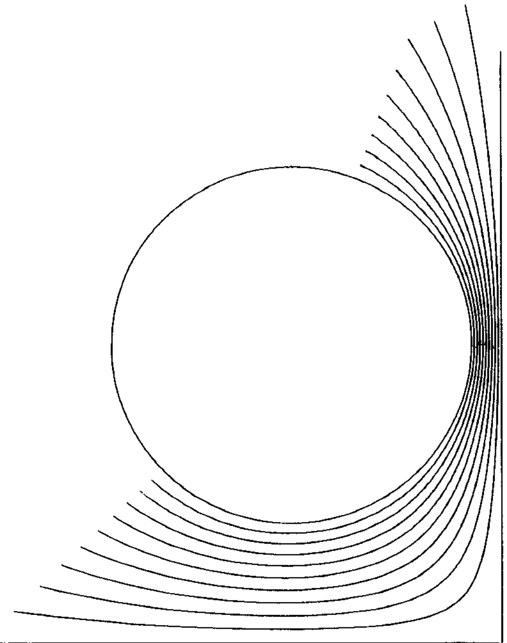

Fig. 5. Equipotential lines in the region of even closer proximity between conductor and wall ($a-A-d=0.5$) on the basis of (12), (A49) with $m=20$.

Finally, in Fig. 5 the equipotentials are plotted for even closer proximity ($a-A-d=0.5$) on the basis of (12), (A49) using $m=20$.

Appendix I

The integrals to be evaluated are defined by the relations (43)–(51). The first, I_1, for $m=0,1,2,\cdots$, is simple:

$$I_1(c, m|A, B) = 2\pi AB\delta_{m0} + \pi Bd\delta_{m1}$$

$$I_1(s, m|A, B) = \pi A d\delta_{m1} + \pi\frac{d^2}{2}\delta_{m2} \tag{A1}$$

where δ_{mn} is the Kronecker delta. The next, I_2, is closely related to the integrals J_2, J_3, J_4, J_5, some of which, but not all, can be evaluated on the basis of standard integrals [16, pp. 487–88]. Here, all will be evaluated by contour integration along the unit circle in the complex plane. To save space we will illustrate the procedure by outlining the steps in the case of the more complicated integrals J_1, J_6–J_9 and P_{mn}^{pq}. For the remaining ones only final results will be provided. So, starting with $J_1(\alpha, \beta|n, c)$ and $J_1(\alpha, \beta|n, s)$ we observe that they are the real and imaginary parts, respectively, of the integral:

$$J_1(\alpha, \beta|n) = \frac{1}{2}\int_0^{2\pi}\ln\left[(\alpha - d\cos\varphi)^2 + (\beta - d\sin\varphi)^2\right]e^{in\varphi}\,d\varphi. \tag{A2}$$

TABLE III

$a_0 = \sigma_0$	a_1	a_2	a_3	a_4	a_5	a_6	a_7	a_8
3.061000	$2.781649\cdot10^{-1}$							
3.072215	$2.725332\cdot10^{-1}$	$-5.166784\cdot10^{-1}$						
3.073703	$2.724612\cdot10^{-1}$	$-5.192405\cdot10^{-1}$	$3.705380\cdot10^{-2}$					
3.073836	$2.725084\cdot10^{-1}$	$-5.195525\cdot10^{-1}$	$3.705042\cdot10^{-2}$	$7.901730\cdot10^{-2}$				
3.073844	$2.725111\cdot10^{-1}$	$-5.195856\cdot10^{-1}$	$3.704676\cdot10^{-2}$	$7.904295\cdot10^{-2}$	$2.668834\cdot10^{-3}$			
3.073845	$2.725111\cdot10^{-1}$	$-5.195893\cdot10^{-1}$	$3.704657\cdot10^{-2}$	$7.904651\cdot10^{-2}$	$2.668804\cdot10^{-3}$	$-7.034012\cdot10^{-3}$		
3.073845	$2.725111\cdot10^{-1}$	$-5.195897\cdot10^{-1}$	$3.704657\cdot10^{-2}$	$7.904703\cdot10^{-2}$	$2.668806\cdot10^{-3}$	$-7.034317\cdot10^{-3}$	$-2.709631\cdot10^{-6}$	
3.073845	$2.725111\cdot10^{-1}$	$-5.195898\cdot10^{-1}$	$3.704657\cdot10^{-2}$	$7.904711\cdot10^{-2}$	$2.668797\cdot10^{-3}$	$-7.034371\cdot10^{-3}$	$-2.454546\cdot10^{-6}$	$8.169953\cdot10^{-4}$

b_1	b_2	b_3	b_4	b_5	b_6	b_7	b_8
-1.412248							
-1.435432	$8.345876\cdot10^{-2}$						
-1.438176	$8.399404\cdot10^{-2}$	$2.274322\cdot10^{-1}$					
-1.438470	$8.397585\cdot10^{-2}$	$2.277107\cdot10^{-1}$	$4.504256\cdot10^{-3}$				
-1.438495	$8.397120\cdot10^{-2}$	$2.277429\cdot10^{-1}$	$4.507281\cdot10^{-3}$	$-2.241980\cdot10^{-2}$			
-1.438498	$8.397109\cdot10^{-2}$	$2.277469\cdot10^{-1}$	$4.5073677\cdot10^{-3}$	$-2.242247\cdot10^{-2}$	$-2.748002\cdot10^{-4}$		
-1.438498	$8.397109\cdot10^{-2}$	$2.277475\cdot10^{-1}$	$4.5073673\cdot10^{-3}$	$-2.242290\cdot10^{-2}$	$-2.748056\cdot10^{-4}$	$2.417227\cdot10^{-3}$	
-1.438498	$8.397108\cdot10^{-2}$	$2.277476\cdot10^{-1}$	$4.5073642\cdot10^{-3}$	$-2.242296\cdot10^{-2}$	$-2.747888\cdot10^{-4}$	$2.417268\cdot10^{-3}$	$1.54900\cdot10^{-5}$

Writing $e^{in\varphi}\,d\varphi = (1/in)\,de^{in\varphi}$, integrating by parts, and observing that, owing to periodicity, the integrated term vanishes, one obtains

$$J_1(\alpha,\beta|n) = \frac{i}{n}\int_0^{2\pi} e^{in\varphi}\frac{\alpha d\sin\varphi - \beta d\cos\varphi}{(\alpha - d\cos\varphi)^2 + (\beta - d\sin\varphi)^2}\,d\varphi \qquad (n>0). \quad \text{(A3)}$$

The change of variable $e^{i\varphi} = \zeta$, $d\zeta = i\zeta\,d\varphi$ leads to a contour integral along $|\zeta| = 1$:

$$\begin{aligned} J_1(\alpha,\beta|n) &= \frac{d}{2n}\oint_{|\zeta|=1}\zeta^{n-1} \cdot \frac{(i\alpha+\beta)\zeta^2 - i\alpha + \beta}{d(\alpha - i\beta)\zeta^2 - (\alpha^2+\beta^2+d^2)\zeta + d(\alpha+i\beta)}\,d\zeta \\ &= \frac{i}{2n}\oint_{|\zeta|=1}\zeta^{n-1}\frac{\zeta^2 - \zeta_1\zeta_2}{(\zeta-\zeta_1)(\zeta-\zeta_2)}\,d\zeta, \end{aligned}$$

$$\zeta_1 = \frac{d}{\alpha - i\beta},\ \zeta_2 = \frac{\alpha + j\beta}{d}. \quad \text{(A4)}$$

For $n>0$ the only pole of the integrand inside $|\zeta| = 1$ is $\zeta = \zeta_1 = d/(\alpha - i\beta)$ since $|\zeta_1\zeta_2| = 1$ and $0 < d < [\alpha^2 + \beta^2]^{1/2}$, as stipulated. Therefore

$$J_1(\alpha,\beta|n) = -\frac{\pi}{n}\zeta_1^n = -\frac{\pi}{n}W^n e^{in\gamma},$$

$$W = \frac{d}{(\alpha^2+\beta^2)^{1/2}} < 1; \qquad \gamma = \tan^{-1}\left(\frac{\beta}{\alpha}\right) \qquad (-\pi < \gamma \leqslant \pi) \quad \text{(A5)}$$

γ being considered a function of the two real variables α, β, not just of their ratio. Finally,

$$J_1\left(\alpha,\beta|n,\frac{c}{s}\right) = -\frac{\pi}{n}W^n\begin{pmatrix}\cos n\gamma\\ \sin n\gamma\end{pmatrix}; \qquad n = 1,2,\cdots \quad \text{(A6)}$$

$$\begin{aligned} J_1(\alpha,\beta|0,c) &= \frac{1}{2}\int_0^{2\pi}\left\{\ln d^2 + \ln\left[1 + \frac{\alpha^2+\beta^2}{d^2} - 2\frac{\alpha}{d}\cos\varphi' - 2\frac{\beta}{d}\sin\varphi'\right]\right\}d\varphi' \\ &= \pi\left[\ln d^2 + \ln\left(\frac{\alpha^2+\beta^2}{d^2}\right)\right] = \pi\ln(\alpha^2+\beta^2), \end{aligned}$$

$$J_1(\alpha,\beta|0,s) = 0. \quad \text{(A7)}$$

The integral of the second logarithmic term was evaluated from standard forms [16, p. 528].

Following similar steps and using the simple results

$$\mathrm{Res}\left[\exp(\alpha\zeta)/\zeta^{n+1}\right]_{\zeta=0} = \alpha^n/n!$$

$$\mathrm{Res}\left[\cos(\alpha\zeta)/\zeta^{n+1}\right]_{\zeta=0} = \begin{cases}(i\alpha)^n/n!, & n = \text{even}\\ 0, & n = \text{odd}\end{cases}$$

$$\mathrm{Res}\left[\sin(\alpha\zeta)/\zeta^{n+1}\right]_{\zeta=0} = \begin{cases}0, & n = \text{even}\\ -i(i\alpha)^n/n!, & n = \text{odd}\end{cases} \quad \text{(A8)}$$

one obtains

$$I_2(c,m|M;\alpha,\beta,\delta)=\pi\epsilon_m\frac{(iM\pi\delta)^m}{m!}\sinh(M\pi\beta)\cdot\begin{bmatrix}\sin(M\pi\alpha), & m=\text{even}\\ -i\cos(M\pi\alpha), & m=\text{odd}\end{bmatrix}\tag{A9}$$

$$I_2(s,m|M;\alpha,\beta,\delta)=-\pi\frac{(iM\pi\delta)^m}{m!}\cosh(M\pi\beta)\cdot\begin{cases}\cos(M\pi\alpha), & m>0 \text{ and even}\\ i\sin(M\pi\alpha), & m=\text{odd}\\ 0, & m=0\end{cases}\tag{A10}$$

where $\epsilon_m=1$ for $m>0$ and $\epsilon_0=2$. Also,

$$J_2\left(M|n,{c \atop s}\right)=-\frac{\pi}{2n!}\begin{pmatrix}i\epsilon_n\\1\end{pmatrix}\left(\frac{iM\pi d}{a}\right)^n\exp\left[-\frac{M\pi}{a}(b-B)\right]\cdot\left[\exp\left(\frac{iM\pi A}{a}\right)\mp(-1)^n\exp\left(-\frac{iM\pi A}{a}\right)\right],\quad J_2(M|0,s)=0\tag{A11}$$

$$J_3\left(M|n,{c \atop s}\right)=\frac{\pi}{2n!}\begin{pmatrix}-i\epsilon_n\\1\end{pmatrix}\left(\frac{iM\pi d}{a}\right)^n\exp\left(-\frac{M\pi B}{a}\right)\cdot\left[\exp\left(\frac{iM\pi A}{a}\right)\mp(-1)^n\exp\left(-\frac{iM\pi A}{a}\right)\right],\quad J_3(M|0,s)=0\tag{A12}$$

$$J_4\left(M|n,{c \atop s}\right)=\frac{\pi}{n!}\left(\frac{M\pi d}{b}\right)^n\exp\left[-\frac{M\pi(a-A)}{b}\right]\cdot\begin{bmatrix}\epsilon_n\sin\left(\frac{M\pi B}{b}\right)\\ \cos\left(\frac{M\pi B}{b}\right)\end{bmatrix},\quad J_4(M|0,s)=0\tag{A13}$$

$$J_5\left(M|n,{c \atop s}\right)=\frac{\pi}{n!}\left(-\frac{M\pi d}{b}\right)^n\exp\left(-\frac{M\pi A}{b}\right)\cdot\begin{bmatrix}\epsilon_n\sin\left(\frac{M\pi B}{b}\right)\\ -\cos\left(\frac{M\pi B}{b}\right)\end{bmatrix},\quad J_5(M|0,s)=0.\tag{A14}$$

There remain the integrals J_6 to J_9 defined in (50), (51). Starting with $J_6(M|n,{c \atop s})$, changing the variables $e^{i\varphi'}=\zeta$, $e^{-i\varphi'}=\eta$ and using the fact that $\exp(\pm iM\pi)=(-1)^M$, one ends up with the following contour integrals along the

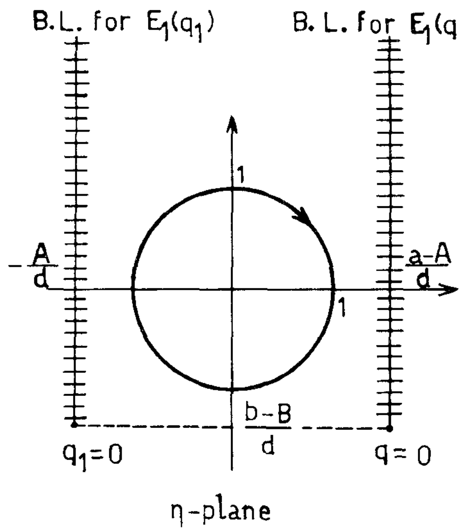

Fig. 6. Cut η plane for contour integration.

unit circles $|\zeta|=1$ and $|\eta|=1$ for $n=1,2\cdots$:

$$J_6\left(M|n,{c \atop s}\right)=\frac{1}{2}\begin{pmatrix}i\\-1\end{pmatrix}\oint_{|\eta|=1}\frac{\eta^{2n}\pm1}{\eta^{n+1}}\cdot\left[(-1)^Me^{q}E_1(q)-e^{q_1}E_1(q_1)\right]d\eta-\frac{1}{2}\begin{pmatrix}i\\1\end{pmatrix}\oint_{|\zeta|=1}\frac{\zeta^{2n}\pm1}{\zeta^{n+1}}\cdot\left[(-1)^Me^{-\bar q}E_1(-\bar q)-e^{-\bar q_1}E_1(-\bar q_1)\right]d\zeta\tag{A15}$$

$$\begin{aligned}q&=i\frac{M\pi d}{a}\left(\eta-\frac{a-A}{d}+i\frac{b-B}{d}\right)\\ q_1&=i\frac{M\pi d}{a}\left(\eta+\frac{A}{d}+i\frac{b-B}{d}\right)\\ -\bar q&=i\frac{M\pi d}{a}\left(\zeta-\frac{a-A}{d}-i\frac{b-B}{d}\right)\\ -\bar q_1&=i\frac{M\pi d}{a}\left(\zeta+\frac{A}{d}-i\frac{b-B}{d}\right).\end{aligned}\tag{A16}$$

The branch points $q=0$, $q_1=0$ in the η plane and the corresponding branch cuts for $E_1(q)$, $E_1(q_1)$ are shown in Fig. 6. Those for $E_1(-\bar q)$, $E_1(-\bar q_1)$ in the ζ plane are shown in Fig. 7. Since $(a-A)/d, A/d, (b-B)/d>1$ all branch points and branch lines lie outside the unit circles $|\eta|=1, |\zeta|=1$. So

$$\begin{aligned}\operatorname{Res}\left[\frac{e^qE_1(q)}{\eta^{n+1}}\right]_{\eta=0}&=\frac{1}{n!}\left\{\frac{d^n}{d\eta^n}[e^qE_1(q)]\right\}_{\eta=0}\\ &=\frac{1}{n!}\left(i\frac{M\pi d}{a}\right)^n\left\{\frac{d^n}{dq^n}[e^qE_1(q)]\right\}_{\eta=0}\\ &=\frac{1}{n!}\left(i\frac{M\pi d}{a}\right)^nF_n(q_0),\end{aligned}$$

$$q_0=q(\eta=0)=-\frac{M\pi}{a}[b-B+i(a-A)].\tag{A17}$$

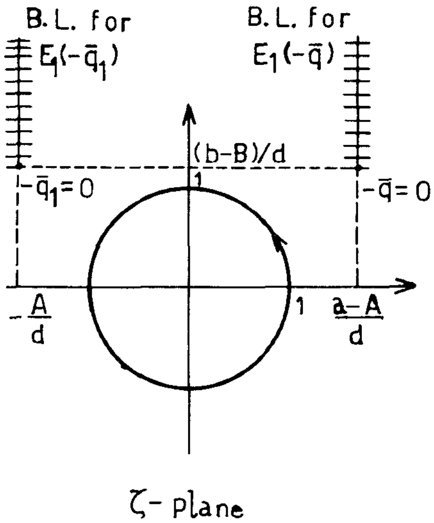

Fig. 7. Cut ζ plane for contour integration.

The function $F_n(q)$ along with a basic recurrence formula it satisfies, taken from [13], is given below:

$$F_n(q) = \frac{d^n}{dq^n}\left[e^q E_1(q)\right]$$
$$= \frac{d^{n-1}}{dq^{n-1}}\left[e^q E_1(q)\right] + \frac{(-1)^n (n-1)!}{q^n}$$
$$= F_{n-1}(q) + \frac{(-1)^n (n-1)!}{q^n},$$
$$n = 1,2,3,\cdots;\; F_0(q) = e^q E_1(q). \quad \text{(A18)}$$

Application of (A17) and the residue theorem to (A15) for $n = 1,2,3\cdots$ yields

$$J_6\left(M|n, {c \atop s}\right) = \frac{\pi}{n!}\begin{pmatrix}1\\-i\end{pmatrix}\left(i\frac{M\pi d}{a}\right)^n \Big\{(-1)^M F_n \cdot\left[-\frac{M\pi}{a}(b-B+i(a-A))\right] - F_n\left[-\frac{M\pi}{a}(b-B-iA)\right] \pm (-1)^M F_n\left[\frac{M\pi}{a}(b-B-i(a-A))\right] \mp F_n\left[\frac{M\pi}{a}(b-B+iA)\right]\Big\}. \quad \text{(A19)}$$

If the recurrence formula of (A18) is applied to the four F_n functions of (A19), we obtain a recurrence formula for J_6 itself:

$$J_6\left(M|n, {c \atop s}\right) = \frac{i}{n}\frac{M\pi d}{a} J_6\left(M|n-1, {c \atop s}\right) + \frac{\pi}{n}\begin{pmatrix}1\\-i\end{pmatrix} \cdot\left[\frac{(-1)^M}{\left(\frac{a-A}{d} - i\frac{b-B}{d}\right)^n} - \frac{(-1)^n}{\left(\frac{A}{d} + i\frac{b-B}{d}\right)^n} \pm \frac{(-1)^M}{\left(\frac{a-A}{d} + i\frac{b-B}{d}\right)^n} \mp \frac{(-1)^n}{\left(\frac{A}{d} - i\frac{b-B}{d}\right)^n}\right]$$
$$= \frac{i}{n}\frac{M\pi d}{a} J_6\left(M|n-1, {c \atop s}\right) + \frac{2\pi}{n}\left[(-1)^M W_1^n \begin{pmatrix}\cos n\gamma_1\\ \sin n\gamma_1\end{pmatrix} \mp (-1)^n W_2^n \begin{pmatrix}\cos n\gamma_2\\ \sin n\gamma_2\end{pmatrix}\right],$$
$$n = 2,3,\cdots \quad \text{(A20)}$$

$$W_1 = \frac{d}{\left[(a-A)^2 + (b-B)^2\right]^{1/2}} < 1$$
$$W_2 = \frac{d}{\left[A^2 + (b-B)^2\right]^{1/2}} < 1$$
$$\gamma_1 = \tan^{-1}\left(\frac{b-B}{a-A}\right)$$
$$\gamma_2 = \tan^{-1}\left(\frac{b-B}{A}\right) \qquad (-\pi < \gamma_1, \gamma_2 \leqslant \pi). \quad \text{(A21)}$$

To start the recurrence formula, a separate evaluation of $J_6(M|1, {c \atop s})$, for $n = 1$, is required. This is obtained from (A19) for $n = 1$. Substituting the four functions $F_1(q)$, appearing in it, by $F_0(q) - 1/q$, with $F_0(q) = e^q E_1(q)$, we finally obtain

$$J_6\left(M|1, {c \atop s}\right) = \begin{pmatrix}i\\1\end{pmatrix}\frac{M\pi^2 d}{a}\Big\{(-1)^M F_0 \cdot\left[-\frac{M\pi}{a}(b-B+i(a-A))\right] - F_0\left[-\frac{M\pi}{a}(b-B-iA)\right] \pm (-1)^M F_0\left[\frac{M\pi}{a}(b-B-i(a-A))\right] \mp F_0\left[\frac{M\pi}{a}(b-B+iA)\right]\Big\} + 2\pi\left[(-1)^M W_1\begin{pmatrix}\cos\gamma_1\\ \sin\gamma_1\end{pmatrix} \pm W_2\begin{pmatrix}\cos\gamma_2\\ \sin\gamma_2\end{pmatrix}\right]. \quad \text{(A22)}$$

There remains the integral $J_6(M|0, c)$, for $n = 0$.

By analogy with (A15), we now obtain simple poles at $\zeta, \eta = 0$ arising only from $d\varphi' = d\zeta/i\zeta$ and $d\varphi' = i\,d\eta/\eta$. Therefore,

$$J_6(M|0,c) = 2\pi\Big\{(-1)^M F_0\Big[-\frac{M\pi}{a}(b-B+i(a-A))\Big] - F_0\Big[-\frac{M\pi}{a}(b-B-iA)\Big] + (-1)^M F_0\Big[\frac{M\pi}{a}(b-B-i(a-A))\Big] - F_0\Big[\frac{M\pi}{a}(b-B+iA)\Big]\Big\}, \qquad J_6(M|0,s) = 0. \tag{A23}$$

The integrals $J_7(M|n,{}^c_s)$ may now be obtained from $J_6(M|n,{}^c_s)$ if $b-B$ in J_6 is replaced everywhere by B and the change of variable $\varphi' = -\varphi$ is introduced in (50), (51). Finally,

$$J_7\Big(M|n,{}^c_s\Big) = \pm J_6\Big(M|n,{}^c_s;\ \text{with } b-B \text{ replaced by } B\Big). \tag{A24}$$

If the two remaining integrals J_8 and J_9 are written out fully, it follows immediately that

$$J_9\Big(M|n,{}^c_s\Big) = J_8\Big(M|n,{}^c_s;\ \text{with } A-a \text{ replaced by } A\Big). \tag{A25}$$

Following the same procedure, we finally end up with

$$J_8\Big(M|n,{}^c_s\Big) = \mp\Big\{\frac{i}{n}\frac{M\pi d}{b}J_8\Big(M|n-1,{}^s_c\Big) - (-1)^n\frac{2\pi}{n}\Big[(-1)^M W_3^n\begin{pmatrix}\cos n\gamma_3\\ \sin n\gamma_3\end{pmatrix} \mp W_4^n\begin{pmatrix}\cos n\gamma_4\\ \sin n\gamma_4\end{pmatrix}\Big]\Big\};\ n = 2,3,\cdots \tag{A26}$$

$$W_3 = \frac{d}{\left[(A-a)^2+(b-B)^2\right]^{1/2}} < 1$$
$$W_4 = \frac{d}{\left[(A-a)^2+B^2\right]^{1/2}} < 1$$
$$\gamma_3 = \tan^{-1}\Big(\frac{b-B}{A-a}\Big)$$
$$\gamma_4 = \tan^{-1}\Big(\frac{B}{A-a}\Big) \qquad (-\pi < \gamma_3, \gamma_4 \leqslant \pi). \tag{A27}$$

Notice that now the recurrence formula relates $J_8(M|n,c)$ and $J_8(M|n,s)$ to $J_8(M|n-1,s)$ and $J_8(M|n-1,c)$, respectively. Again the functions $\gamma = \tan^{-1}(\beta/\alpha)$ depend on both the real variables α, β, not just on their ratio. For $n=1$ and $n=0$, we also have

$$J_8\Big(M|1,{}^c_s\Big) = \Big(\frac{-1}{i}\Big)\frac{M\pi^2 d}{b}\Big\{(-1)^M F_0\Big[-\frac{M\pi}{b}(A-a+i(b-B))\Big] - F_0\Big[-\frac{M\pi}{b}(A-a-iB)\Big] \mp(-1)^M F_0\Big[\frac{M\pi}{b}(A-a-i(b-B))\Big] \pm F_0\Big[\frac{M\pi}{b}(A-a+iB)\Big]\Big\} - 2\pi\Big[\pm(-1)^M W_3\begin{pmatrix}\cos\gamma_3\\ \sin\gamma_3\end{pmatrix} - W_4\begin{pmatrix}\cos\gamma_4\\ \sin\gamma_4\end{pmatrix}\Big] \tag{A28}$$

$$J_8(M|0,c) = 2\pi\Big\{(-1)^M F_0\Big[-\frac{M\pi}{b}(A-a+i(b-B))\Big] - F_0\Big[-\frac{M\pi}{b}(A-a-iB)\Big] + (-1)^M F_0\Big[\frac{M\pi}{b}(A-a-i(b-B))\Big] - F_0\Big[\frac{M\pi}{b}(A-a+iB)\Big]\Big\};$$
$$J_8(M|0,s) = 0. \tag{A29}$$

All the integrals evaluated in this appendix have also been checked to very high accuracy (five significant decimals) by numerical integration. Furthermore, it is easy to verify that the series over M in (52) converge exponentially with M, unless the inner conductor is located very near the shield boundary. In this latter case the expressions of Appendix II may be used instead.

The last integral to be evaluated, P_{mn}^{pq}, is defined in (68). From Fig. 2 and (62),

$$\ln R(\varphi,\varphi'') = \ln r(\varphi) - \sum_{N=1}^{\infty}\frac{1}{N}\Big(\frac{d}{r}\Big)^N\cos\left[N(\varphi''-\omega)\right] = \ln r(\varphi) - \sum_{N=1}^{\infty}\frac{1}{N}\Big(\frac{d}{r}\Big)^N \cdot(\cos N\varphi''\cos N\omega + \sin N\varphi''\sin N\omega) \tag{A30}$$

where ω, r are functions of φ only. Therefore,

$$\int_0^{2\pi}\ln R(\varphi,\varphi'')\begin{pmatrix}\cos n\varphi''\\ \sin n\varphi''\end{pmatrix}d\varphi'' = \begin{cases} -\dfrac{\pi}{n}\Big(\dfrac{d}{r}\Big)^n\begin{pmatrix}\cos n\omega\\ \sin n\omega\end{pmatrix}, & n = 1,2,\cdots \\ 2\pi\ln r(\varphi)\begin{pmatrix}1\\0\end{pmatrix}, & n = 0.\end{cases} \tag{A31}$$

For $n=0$ we refer again to Fig. 2 and expand:

$$\ln r(\varphi) = \ln(2A-a) - \sum_{N=1}^{\infty}\frac{1}{N}\Big(\frac{d}{2A-a}\Big)^N(-1)^N\cos N\varphi. \tag{A32}$$

Substituting (A36) and (A37) into (68), we get

$$P_{00}^{pq} = 4\ln(2A-a)\delta_{pc}\delta_{qc}$$

$$(\delta_{pq}=1 \text{ if } p=q,\ \delta_{pq}=0 \text{ if } p\neq q) \quad \text{(A33)}$$

$$P_{m0}^{pq} = -\frac{2}{m}(-1)^m\left(\frac{d}{2A-a}\right)^m\delta_{pc}\delta_{qc}$$

$$(m=1,2,\cdots). \quad \text{(A34)}$$

For $n=1,2,\cdots$ we consider the integral

$$P_{mn}^{p} = -\frac{1}{\pi n}\int_0^{2\pi}\begin{pmatrix}\cos m\varphi; & p=c\\ \sin m\varphi; & p=s\end{pmatrix}\left[\frac{d}{r(\varphi)}\right]^n e^{-in\omega(\varphi)}\,d\varphi \quad \text{(A35)}$$

so that $P_{mn}^{pc}=\operatorname{Re}P_{mn}^{p}$ and $P_{mn}^{ps}=-\operatorname{Im}P_{mn}^{p}$. From Fig. 2, $re^{i\omega}=2A-a+de^{i\varphi}$ and $(re^{i\omega})^{-n}=1/(2A-a+de^{i\varphi})^n$.

The change of variable $e^{i\varphi}=\zeta$ leads to

$$P_{mn}^{p} = -\frac{1}{2\pi in}\oint_{|\zeta|=1}\begin{bmatrix}\zeta^m+\zeta^{-m}; & p=c\\ -i(\zeta^m-\zeta^{-m}); & p=s\end{bmatrix}\cdot\frac{1}{\left(\zeta-\dfrac{a-2A}{d}\right)^n}\frac{d\zeta}{\zeta} \quad (m=1,2,\cdots) \quad \text{(A36)}$$

$$P_{0n}^{p} = -\frac{1}{\pi in}\oint_{|\zeta|=1}\frac{d\zeta}{\zeta\left(\zeta-\dfrac{a-2A}{d}\right)^n}\delta_{pc} \quad (m=0). \quad \text{(A37)}$$

The pole at $\zeta=(a-2A)/d$ is exterior to the unit circle, as seen from Fig. 2. Only the pole at $\zeta=0$ is inside. Therefore,

$$P_{0n}^{pq} = -\frac{2}{n}\left(\frac{d}{2A-a}\right)^n\delta_{pc}\delta_{qc} \quad \text{(A38)}$$

while for $m=1,2,\cdots$

$$P_{mn}^{p} = -\frac{1}{\pi m!}\begin{pmatrix}1; & p=c\\ i; & p=s\end{pmatrix}\left\{\frac{d^m}{d\zeta^m}\left[\left(\zeta-\frac{a-2A}{d}\right)^{-n}\right]\right\}_{\zeta=0}$$

$$= -\frac{1}{n}\begin{pmatrix}1; & p=c\\ i; & p=s\end{pmatrix}\binom{m+n-1}{m}(-1)^m\cdot\left(\frac{2A-a}{d}\right)^{-n-m}.$$

Finally, for $n,m=1,2,\cdots$

$$P_{mn}^{pc} = -\delta_{pc}\frac{(-1)^m}{n}\binom{m+n-1}{m}\left(\frac{d}{2A-a}\right)^{m+n}$$

$$P_{mn}^{ps} = \delta_{ps}\frac{(-1)^m}{n}\binom{m+n-1}{m}\left(\frac{d}{2A-a}\right)^{m+n}. \quad \text{(A39)}$$

Observe that, although $\binom{m+n-1}{n}$ increases with m and n, $d/(2A-a)<1/2$. Using Stirling's formula [13, p. 257],

$$x! = \sqrt{2\pi}\,x^{x+1/2}\exp(-x+\theta/12x) \quad (x>0,\ 0<\theta<1) \quad \text{(A40)}$$

we obtain, for large m,n,

$$|P_{mn}^{pq}| < \frac{et_{mn}}{[2\pi mn(m+n-1)]^{1/2}},\quad t_{mn}=\left(\frac{m+n-1}{2m}\right)^m\left(\frac{m+n-1}{2n}\right)^n. \quad \text{(A41)}$$

It is easy to show that $et_{mn}<1$. Without loss of generality, we may assume $m=n+s$ $(s\geq 0)$. Then

$$\ln t_{mn} = (n+s)\ln\left[1-\frac{s+1}{2(n+s)}\right]+n\ln\left(1+\frac{s-1}{2n}\right) < -\frac{s+1}{2}+\frac{s-1}{2}=-1.$$

Therefore, $\ln t_{mn}<-1$ or $t_{mn}<1/e$. We made use of the well-known inequalities [13, p. 68]

$$\frac{x}{1+x}<\ln(1+x)<x$$

$$(x>-1,\ x\neq 0) \quad \text{and} \quad \frac{x}{x-1}<\ln(1-x)<-x$$

$$(x<1,\ x\neq 0).$$

For $s=0,1$ it is obvious that $t_{mn}<1$. Therefore, $|P_{mn}^{pq}|$ varies at least proportionally to $[mn(m+n-1)]^{-1/2}$.

Appendix II

Based on the expansion (12) for G, the expression equivalent to (52) for K_{mn}^{pq} is

$$\begin{aligned}K_{mn}^{pq} = -\frac{1}{\pi^2 ab}&[I_1(p,m|A,B)J_1(-a-A,b-B|n,q)\\ &-I_1(p,m|A-a,B)J_1(2a-A,b-B|n,q)\\ &-I_1(p,m|A,B-b)J_1(-a-A,-B|n,q)\\ &+I_1(p,m|A-a,B-b)J_1(2a-A,-B|n,q)]\\ &+T_{mn}^{pq}+\sum_{M=1}^{\infty}\left\{\frac{I_2\left(p,m|M;\frac{A}{a},\frac{B}{a},\frac{d}{a}\right)}{M\pi^3\sinh\left(\frac{M\pi b}{a}\right)}\right.\\ &\cdot[-2\pi J_2(M|n,q)-\operatorname{Re}J_6(M|n,q)\\ &+\operatorname{Re}J_{10}(M|n,q)+\operatorname{Re}J_{11}(M|n,q)]\\ &-\frac{I_2\left(p,m|M;\frac{A}{a},\frac{B-b}{a},\frac{d}{a}\right)}{M\pi^3\sinh\left(\frac{M\pi b}{a}\right)}[-2\pi J_3(M|n,q)\\ &-\operatorname{Re}J_7(M|n,q)+\operatorname{Re}J_{12}(M|n,q)\\ &+\operatorname{Re}J_{13}(M|n,q)]-\frac{I_2\left(p,m|iM;\frac{A}{b},\frac{B}{b},\frac{d}{b}\right)}{M\pi^3\sinh\left(\frac{M\pi a}{b}\right)}\\ &\cdot[2\pi J_5'(M|n,q)+\operatorname{Re}J_{14}(M|n,q)]\\ &+\frac{I_2\left(p,m|iM;\frac{A-a}{b},\frac{B}{b},\frac{d}{b}\right)}{M\pi^3\sinh\left(\frac{M\pi a}{b}\right)}[2\pi J_4'(M|n,q)\\ &\left.+\operatorname{Re}J_{15}(M|n,q)]\right\},\quad (p,q=c,s \text{ or } s,c),\end{aligned}$$

$$m,n=0,1,2,\cdots. \quad \text{(A42)}$$

The definitions and values of the additional integrals appearing here are

$$T_{mn}^{pq}=\frac{1}{2\pi^2}\int_0^{2\pi}\int_0^{2\pi}\begin{pmatrix}\cos m\varphi; & p=c\\ \sin m\varphi; & p=s\end{pmatrix}\Big\{\ln\big[(2A-2a+d\cos\varphi+d\cos\varphi')^2+(d\sin\varphi-d\sin\varphi')^2\big]$$
$$+\ln\big[(2A+d\cos\varphi+d\cos\varphi')^2+(d\sin\varphi-d\sin\varphi')^2\big]\Big\}\begin{pmatrix}\cos n\varphi'; & q=c\\ \sin n\varphi'; & q=s\end{pmatrix}d\varphi\,d\varphi' \quad \text{(A43)}$$

$$T_{mn}^{pc}=-\delta_{pq}\left[\frac{1}{m}\binom{m+n-1}{n}\left(\frac{d}{2a-2A}\right)^{m+n}+\frac{(-1)^{m+n}}{n}\binom{m+n-1}{m}\left(\frac{d}{2A}\right)^{m+n}\right],$$
$$m,n=1,2,\cdots \quad \text{(A44)}$$

$$T_{0n}^{pq}=-\frac{2}{n}\delta_{pc}\delta_{qc}\left[\left(\frac{d}{2a-2A}\right)^{n}+(-1)^{n}\left(\frac{d}{2A}\right)^{n}\right],$$
$$n=1,2,\cdots \quad \text{(A45)}$$

$$T_{m0}^{pq}=-\frac{2}{m}\delta_{pc}\delta_{qc}\left[\left(\frac{d}{2a-2A}\right)^{m}+(-1)^{m}\left(\frac{d}{2A}\right)^{m}\right],$$
$$m=1,2,\cdots \quad \text{(A46)}$$

$$T_{00}^{pq}=4\delta_{pc}\delta_{qc}[\ln(2a-2A)+\ln(2A)] \quad \text{(A47)}$$

$$J_{10}\left(M|n,{c\atop s}\right)=\pm J_6\left(M|n,{c\atop s};a\to -a,A\to A-2a,\; b-B\to-(b-B)\right)$$
$$J_{11}\left(M|n,{c\atop s}\right)=\pm J_6\left(M|n,{c\atop s};a\to -a,b-B\to-(b-B)\right)$$
$$J_{12}\left(M|n,{c\atop s}\right)=J_6\left(M|n,{c\atop s};a\to -a,A\to A-2a,\; b-B\to -B\right)$$
$$J_{13}\left(M|n,{c\atop s}\right)=J_6\left(M|n,{c\atop s};a\to -a,b-B\to -B\right) \quad \text{(A48)}$$
$$J_{14}\left(M|n,{c\atop s}\right)=J_8\left(M|n,{c\atop s};A-a\to a+A\right)$$
$$J_{15}\left(M|n,{c\atop s}\right)=J_8\left(M|n,{c\atop s};A-a\to -2a+A\right)$$
$$J_4'\left(M|n,{c\atop s}\right)=J_4\left(M|n,{c\atop s};A\to -a+A\right)$$
$$J_5'\left(M|n,{c\atop s}\right)=J_5\left(M|n,{c\atop s};A\to a+A\right)$$

where $a\to A$ means replacement of a by A. Finally, the expression $D(x,y|n,{c\atop s})$ appearing in (53) for the potential $\psi(x,y)$, evaluated on the basis of (12) for G, takes the form

$$D\left(x,y|n,{c\atop s}\right)=J_1\left(x-A,y-B|n,{c\atop s}\right)-J_1\left(2a-x-A,\; y-B|n,{c\atop s}\right)-J_1\left(-x-A,y-B|n,{c\atop s}\right)$$
$$+\frac{1}{ab}\Big[xyJ_1\left(-a-A,b-B|n,{c\atop s}\right)+(a-x)yJ_1\left(2a-A,b-B|n,{c\atop s}\right)$$
$$+x(b-y)J_1\left(-a-A,-B|n,{c\atop s}\right)+(a-x)(b-y)J_1\left(2a-A,-B|n,{c\atop s}\right)\Big]$$
$$-\sum_{M=1}^{\infty}\frac{\sin\left(\frac{M\pi x}{a}\right)\sinh\left(\frac{M\pi y}{a}\right)}{M\pi\sinh\left(\frac{M\pi b}{a}\right)}\cdot\Big[-2\pi J_2\left(M|n,{c\atop s}\right)-\operatorname{Re}J_6\left(M|n,{c\atop s}\right)+\operatorname{Re}J_{10}\left(M|n,{c\atop s}\right)+\operatorname{Re}J_{11}\left(M|n,{c\atop s}\right)\Big]$$
$$-\sum_{M=1}^{\infty}\frac{\sin\left(\frac{M\pi x}{a}\right)\sinh\left[\frac{M\pi}{a}(b-y)\right]}{M\pi\sinh\left(\frac{M\pi b}{a}\right)}\cdot\Big[-2\pi J_3\left(M|n,{c\atop s}\right)-\operatorname{Re}J_7\left(M|n,{c\atop s}\right)+\operatorname{Re}J_{12}\left(M|n,{c\atop s}\right)+\operatorname{Re}J_{13}\left(M|n,{c\atop s}\right)\Big]$$
$$-\sum_{M=1}^{\infty}\frac{\sin\left(\frac{M\pi y}{b}\right)\sinh\left(\frac{M\pi x}{b}\right)}{M\pi\sinh\left(\frac{M\pi a}{b}\right)}\cdot\Big[2\pi J_5'\left(M|n,{c\atop s}\right)+\operatorname{Re}J_{14}\left(M|n,{c\atop s}\right)\Big]$$
$$-\sum_{M=1}^{\infty}\frac{\sin\left(\frac{M\pi y}{b}\right)\sinh\left[\frac{M\pi(a-x)}{b}\right]}{M\pi\sinh\left(\frac{M\pi a}{b}\right)}\cdot\Big[2\pi J_4'\left(M|n,{c\atop s}\right)+\operatorname{Re}J_{15}\left(M|n,{c\atop s}\right)\Big]. \quad \text{(A49)}$$

References

[1] T. C. Edwards, *Foundations for Microstrip Circuit Design*. New York: Wiley, 1981.

[2] N G. Alexopoulos, "Integrated-circuit structures on anisotropic substrates," *IEEE Trans. Microwave Theory Tech.*, vol. MTT-33, pp. 847–881, Oct. 1985.

[3] E. G. Cristal, "Coupled circular cylindrical rods between parallel ground planes," *IEEE Trans. Microwave Theory Tech.*, vol. MTT-12, pp. 428–439, July 1964.

[4] R. Levy, "Conformal transformations combined with numerical techniques, with applications to coupled-bar problems," *IEEE Trans. Microwave Theory Tech.*, vol. MTT-28, pp. 369–375, Apr. 1980.

[5] R. Levy, "Direct noniterative numerical solution of field theory problems having irregular boundaries using network analogs," *IEEE Trans. Microwave Theory Tech.*, vol. MTT-28, pp. 596–604, June 1980.
[6] J. G. Fikioris, "On the convergence of orthogonal eigenfunction series," *Math. Comp. Simul.*, vol. 27, pp. 531–539, 1985.
[7] J. G. Fikioris and J. L. Tsalamengas, "Strongly and uniformly convergent Green's function expansions," *J. Franklin Inst.*, vol. 324, no. 1, pp. 1–17, 1987.
[8] J. G. Fikioris, J. L. Tsalamengas, and G. J. Fikioris, "Strongly convergent Green's function expansions for rectangularly shielded microstrip lines," submitted to *IEEE Trans. Microwave Theory Tech.*
[9] J. G. Fikioris, J. L. Tsalamengas, and G. J. Fikioris, "Exact solutions for shielded printed microstrip lines by the Carleman–Vekua method," submitted to *IEEE Trans. Microwave Theory Tech.*
[10] F. D. Gakhov, *Boundary Value Problems* (translation by I. N. Sneddon). Oxford: Pergamon Press, 1966.
[11] L. Lewin, "The use of singular integral equations in the solution of waveguide problems," *Advances in Microwaves*, vol. 1, L. Young, Ed. New York: Academic Press, 1966, pp. 212–284.
[12] R. Mittra and T. Itoh, "A new technique for the analysis of the dispersion characteristics of microstrip lines," *IEEE Trans. Microwave Theory Tech.*, vol. MTT-19, pp. 47–56, Jan. 1971.
[13] M. Abramowitz and I. A. Stegun, *Handbook of Mathematical Functions*. New York, Dover, 1972.
[14] D. M. Pozar, "A useful decomposition for the Green's functions of cylinders and spheres," *Radio Sci.*, vol. 17, no. 5, pp. 1192–1198, Sept.–Oct. 1982.
[15] R. P. Kanwal, *Linear Integral Equations, Theory and Technique*. New York: Academic Press, 1971.
[16] I. S. Gradshteyn and I. M. Ryzhik, *Tables of Integrals, Series and Products*, 4th ed. (English translation by A. Jeffrey). New York: Academic Press, 1965.

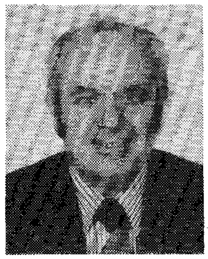

John G. Fikioris was born in Sparta, Greece, on April 9, 1931. He received the Diploma in electrical engineering and mechanical engineering from the National Technical University of Athens, Greece, in 1955, the M.S.E.E. degree from the Rensselaer Polytechnic Institute, Troy, NY, in 1958, and the M.A. and Ph.D. degrees in applied physics from Harvard University, Cambridge, MA, in 1963.

From 1962 until early 1966, he worked as a Research Scientist with the R&D division of Avco Corporation, Wilmington, MA. From January 1966 to June 1972, he was Professor of Electrical Engineering at the University of Toledo, OH. In May 1972, he was elected Professor of Wireless and Long Distance Communications at the National Technical University of Athens, a position that he holds to date. His research contributions include topics in guiding phenomena, wave optics, antennas and wave propagation, diffraction and scattering, fundamental electromagnetic theory, and special mathematical techniques in applied electromagnetics.

Dr. Fikioris is a member of Sigma Xi.

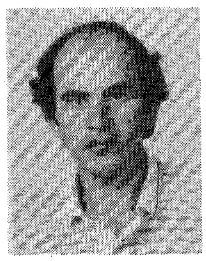

John L. Tsalamengas (M'87) was born in Karditsa, Greece, on April 26, 1953. He received the Diploma of electrical and mechanical engineering and the doctor's degree in electrical engineering from the National Technical University of Athens (N.T.U.A.), Greece, in 1977 and 1983, respectively.

In 1983 he joined the Hellenic Aeorspace Academy and worked there until the end of 1984. He then joined the Department of Electrical Engineering at the N.T.U.A., first as a Research Associate and then, in July 1987, as Assistant Professor of Electrical Engineering. His fields of interest include waveguide propagation, printed microwave (microstrip) devices, and boundary value problems in electromagnetic theory.